

Type of article: Forum Original Research Communication

Title: Evidence for constitutive microbiota-dependent short-term control of food intake in mice: Is there a link with inflammation, oxidative stress, endotoxemia, and Glp-1?

Running title: Microbial control of food intake

Contributing Authors: Selma Ben Fradj¹, Emmanuelle Nédélec¹, Juliette Salvi¹, Mélanie Fouesnard^{2,9}, Marine Huillet³, Gaëtan Pallot⁴, Céline Cansell⁵, Clara Sanchez⁵, Catherine Philippe², Vincent Gigot¹, Aleth Lemoine¹, Doriane Trompier¹, Thomas Henry⁶, Virginie Petrilli⁷, Benedicte F. Py⁶, Hervé Guillou³, Nicolas Loiseau³, Sandrine Ellero-Simatos³, Jean-Louis Nahon⁵, Carole Rovère⁵, Jacques Grober⁴, Gaelle Boudry^{#,8}, Véronique Douard^{#,2}, Alexandre Benani^{#,*,1}

[#]Equal contribution

*Correspondence: Dr. Alexandre Benani, alexandre.benani@u-bourgogne.fr

Affiliations:

1. CSGA, Centre des Sciences du Goût et de l'Alimentation, CNRS (UMR6265), INRAE (UMR1324), Institut Agro Dijon, Université Bourgogne Franche-Comté, Dijon, France
2. Institut Micalis, INRAE (UMR1319), AgroParisTech, Université Paris-Saclay, Jouy-en-Josas, France
3. Toxalim (Research Centre in Food Toxicology), Université de Toulouse 3, INRAE (UMR1331), ENVT, INP-Purpan, Université Paul Sabatier, Toulouse, France
4. Centre de Recherche Lipides, Nutrition, Cancer, INSERM (UMR1231), Institut Agro Dijon, Université Bourgogne Franche-Comté, Dijon, France
5. IPMC, Institut de Pharmacologie Moléculaire et Cellulaire, CNRS (UMR7275), Université Côte d'Azur, Valbonne, France

6. CIRI, Centre International de Recherche en Infectiologie, Inserm (U1111), CNRS (UMR5308), ENS de Lyon, Université Claude Bernard Lyon 1, Lyon, France
7. Centre de Recherche en Cancérologie de Lyon, Inserm (U1052), CNRS (UMR5286), Université de Lyon 1, Lyon, France
8. Institut NuMeCan, INRAE (UMR1341), INSERM (UMR1241), Université de Rennes 1, St-Gilles, France

Keywords: Energy homeostasis, food intake, satiety, eating disorders, microbiota, gut.

Word count: 5227 (excluding Figure Legends, References, and Materials and Methods)

Number of references: 93

Number of greyscale figures: 0

Number of color figures: 9

Number of supplemental color figures: 6

Abstract

Aims: Although prebiotics, probiotics, and fecal transplantation can alter the sensation of hunger and/or feeding behavior, the role of the constitutive gut microbiota in the short-term regulation of food intake during normal physiology is still unclear.

Results: An antibiotic-induced microbiota depletion study was designed to compare feeding behavior in conventional and microbiota-depleted mice. Tissues were sampled to characterize the time profile of microbiota-derived signals in mice during consumption of either standard or high-fat food for 1 hour. Pharmacological and genetic tools were used to evaluate the contribution of postprandial endotoxemia and inflammatory responses in the short-term regulation of food intake. We observed constitutive microbial and macronutrient-dependent control of food intake at the time scale of a meal, i.e., within 1 hour of food introduction. Specifically, microbiota depletion increased food intake and the microbiota-derived anorectic effect became significant during the consumption of high-fat but not standard food. This anorectic effect correlated with a specific postprandial microbial metabolic signature and did not require postprandial endotoxemia or an NLRP3 (NOD-, LRR- and Pyrin domain-containing protein 3)-inflammasome mediated inflammatory response.

Innovation and Conclusion: These findings show that the gut microbiota controls host appetite at the time scale of a meal under normal physiology. Interestingly, a microbiota-derived anorectic effect develops specifically with a high-fat meal, indicating that gut microbiota activity is involved in the satietogenic properties of foods.

Introduction

The gut is inhabited by trillions of microbes, which directly influence host metabolism and health (88). It has recently been proposed that the gut microbiota influences food intake (2,34,52,89). Actually, dietary prebiotic supplementation can reduce food intake (5,6,18,47,53). Moreover, some probiotics can alter appetite in humans and change feeding behavior in laboratory animals (7,33,50,60,82). Fecal microbiota transplantation can also modify food intake (86). Several non-exclusive mechanisms have been proposed to explain the regulatory effect of the gut microbiota on feeding behavior. Strikingly, dietary prebiotic and probiotic supplementation studies show a strong correlation between gut microbiota activity and the release of gastrointestinal peptides involved in appetite regulation (17,29,39). Furthermore, specific microbiota-derived molecules are known to be gut hormone-releasing factors (58,87). In addition, the gut microbiota produces neuroactive peptides that modulate the activity of the enteric nervous system, which is notably involved in the control of food intake (55). Moreover, bacterial toxins, such as lipopolysaccharide (LPS), the plasma concentration of which is closely associated to energy intake, can activate vagal afferent terminals and alter their sensitivity to leptin (3,28,37). Circulating bacterial molecules might also directly activate brain areas that control appetite. For instance, it has been suggested that gut microbiota-derived acetate reduces appetite after reaching central homeostatic feeding centers (36). Finally, recent studies revealed the existence of microbiota molecular mimetics that might act on receptors expressed in the brain and thus impact behavior (34,77). Indeed, the caseinolytic protease B (ClpB) is a mimetic of the host α -melanocyte-stimulating hormone (α -MSH), and is able to activate anorectic POMC (pro-opiomelanocortin) neurons within the hypothalamus (11).

Experimental and clinical manipulations of gut microbiota by prebiotics, probiotics, fecal transplantations, or nutritional interventions, and dysbioses found during obesity, diabetes, and anorexia nervosa clearly support a relationship between microbes and host feeding behavior. However, the role of the constitutive gut microbiota on food intake under normal physiology, i.e. without preliminary microbiota manipulation and in a non-disease state, remains to be defined. Moreover, the exact role of the constitutive gut microbiota on appetite and satiety, if any, has not been elucidated. In addition, mechanistic studies have

determined diverse neuroendocrine routes in the gut-brain axis that microbiota-derived signals probably use to affect food intake. Notably, this includes gut inflammatory/oxidative stress, systemic endotoxemia, and glucagon-like peptide-1 (GLP-1). Nevertheless, it is still unclear whether these relays that are involved in the host response to a modified microbiota are also engaged by the constitutive microbiota to trigger a behavioral response under normal conditions.

In an antibiotic-induced microbiota depletion study, we show the role of the constitutive gut microbiota in the short-term regulation of food intake. In addition, we describe the time profile of microbiota-derived signals in mice, over the course of a meal, during consumption of either a standard diet (SD) or a high-fat diet (HFD). We show that the gut microbiota can modulate food intake according to food composition. Specifically, the microbiota-derived anorectic effect of the gut microbiota is apparent during consumption of HFD during 1 hour but not SD. Moreover, this anorectic effect correlates with a specific postprandial microbial metabolic signature. Conversely, molecular, pharmacological and genetic studies do not support a role for postprandial NLRP3-dependent inflammation, gut oxidative stress, TLR4 signaling, and GLP-1 release in the ABX-sensitive behavioral effects that develop within 1 hour (Figure 1).

Results

The microbiota is involved in the short-term regulation of food intake when consuming high-fat food.

To assess the role of the microbiota on the short-term regulation of food intake, we examined feeding behavior in microbiota-depleted and control mice. To deplete microbes prior to behavioral analyses, a mix of antibiotics (ABX) was given orally in drinking water for 2 weeks, while control mice received no treatment (Figure 2A). The ABX treatment dramatically increased the size of the cecum, the content of which became dark, and strongly reduced DNA content and bacterial 16S rRNA gene copy number in feces (Figure 2B-E), indicating effective gut microbiota depletion in ABX-treated mice. Moreover, fecal cultures prepared from control and ABX-treated mice revealed no colony-forming units of viable aerobic bacteria in the ABX group and confirmed that ABX resulted in microbiota depletion in the gut. Importantly, the ABX treatment did not alter food intake and body

weight as measured under standard diet over the 24h prior acute feeding tests (Figure S1A) and did not cause discomfort, clinical symptoms or mortality. A few episodic decreases in daily water intake were observed during ABX treatment, but these were normalized prior to the analyses (Figure S1A). In addition, ABX treatment did not alter mRNA expression of interleukin 1 beta (IL-1 β) and cyclooxygenase-2 (COX-2), two pro-inflammatory markers, while it markedly down-regulated expression of tumor necrosis factor alpha (TNF α ; Figure S1B). Notably, ABX treatment did not change the mRNA expression of a set of redox markers in the gut, including the anti-inflammatory and antioxidant transcription factor nuclear factor erythroid 2-related factor 2 (NRF2), and the two antioxidant enzymes: catalase (CAT) and superoxide dismutase-1 (SOD). Thus, the ABX treatment *per se* did not initiate gut inflammation or oxidative stress.

Mice were then fed either a standard or a high-fat diet (SD or HFD) and feeding behavior was monitored for 1 hour during the active period of the mice, at the onset of the night period (Figures S1C, S1D). ABX had no effect on feeding behavior in mice fed a SD for 1 hour (Figure 2G). In contrast, ABX increased HFD food intake over the 1-hour period (Figure 2H). This increase in food consumption for the microbiota-depleted mice fed HFD was explained by a higher number of feeding bouts without any change in the size or duration of these bouts. As a result, the time spent feeding was markedly increased in ABX-treated mice on HFD compared to controls, with consequently reduced inter-bout intervals. These results reveal a constitutive ABX-sensitive short-term control of food intake that develops during a high fat meal, supporting the existence of a macronutrient-dependent release of microbiota-derived satietogenic signals.

HFD changes the cecal microbial metabolic signature at the time scale of a meal.

Feeding behavior in microbiota-depleted mice varied depending on the type of food ingested (SD or HFD). To determine the source of this differentiation, we first investigated postprandial changes in microbial metabolites produced in the cecum during SD and HFD consumption in non-ABX-treated mice. Levels of cecal short chain fatty acids (SCFA) were analyzed by gas chromatography. While consumption of SD did not significantly change SCFA concentration in the cecum compared to the preprandial state, HFD briefly increased cecal branched SCFA, and isovalerate in particular, after 20 minutes (Figure 3). In addition,

the level of total SCFA was reduced after 1 hour of HFD feeding compared to SD. This is largely explained by the reduction in acetate and propionate levels. These data show that the postprandial microbial metabolic signature varies according to the type of ingested diet.

Postprandial GLP-1 response varies according to food composition.

During food consumption, the endocrine gut releases several hormones that stimulate meal termination and satiety. The gut microbiota has been shown to modulate the release of endogenous stores of gut hormones into the blood (40). Before examining the effect of ABX treatment on the postprandial release of gut hormones in our model, we first monitored the postprandial GLP-1 response as an indicator of gut hormone pathway activation. As expected, plasma levels of total GLP-1 increased in mice after consumption of SD (Figure 4). This release was further increased after HFD consumption, indicating differences in hormonal signaling that are dependent on food composition.

HFD induces a pro-inflammatory response in the gut at the time scale of a meal.

Gut microbiota is a critical inducer of immune responses, and the immune system constitutes one of the routes of communication for the gut-brain axis (9,26,44). Gut-associated immune cells are components of this system and contribute to the maintenance of tissue homeostasis. Thus, we assessed the abundance of CD4-positive and CD8-positive T lymphocytes and F4/80-positive macrophages in histological tissue sections of intestine from mice fed SD or HFD for 1 hour (Figure S2). We found that SD consumption increased CD4 immunostaining in the small intestine, suggesting the recruitment of CD4-positive T cells in the gut after a balanced meal (Figure 5A). A slight increase in CD8 and F4/80 staining was also observed in some intestinal segments after 1h-SD, but it remained below the significance threshold in most cases suggesting that immune cells were not recruited in the gut for 1h-HFD. Instead, samples from HFD-fed mice had reduced F4/80 staining in the jejunum and the colon, suggesting withdrawal of gut macrophages after HFD ingestion. More generally, these observations suggest reduced immune defense in the gut following HFD consumption.

Inflammatory molecules that are released in the intestinal microenvironment dictate immunological reactions and propagate inflammatory responses (72). We investigated the

postprandial regulation of key inflammatory markers in intestinal tissues of mice fed SD or HFD for 1 hour. Expression levels of IL-1 β , TNF α , and COX-2 mRNA were significantly increased in both the jejunum and duodenum after HFD consumption (Figure 5B). No changes were detected in distal parts of the gut. Taken together, these data indicate specific postprandial immune responses in the gut as a function of the type of diet ingested and support the idea that HFD consumption induces local pro-inflammatory responses.

We also assessed the postprandial regulation of the key redox markers in the intestines of mice fed SD or HFD for 1 hour, including NRF2, CAT and SOD. Analyses revealed some changes in the duodenum but not in distal parts of the gut (Figure 5C). NRF2 was up-regulated after 1h-HFD, but not after SD, and conversely, CAT was upregulated in response to SD but not HFD. These data suggest rapid postprandial changes in redox homeostasis in the upper parts of the gut.

HFD induces a systemic inflammatory response at the time scale of a meal.

Next, we compared the systemic postprandial inflammatory response in mice fed SD or HFD for 1 hour by measuring plasma level of several inflammatory factors. Biochemical analyses revealed a rapid and sustained elevation of the chemokine CCL5 (alias RANTES) in the plasma, 20 minutes after the introduction of HFD food, but not after SD feeding (Figure 6). HFD, but not SD, consumption also increased plasma levels of IL-1 β , IL-6 and TNF α within 1 hour. Plasma levels of other factors such as CCL2 (alias MCP1), IL-10 and IFN γ were not affected after feeding, regardless of the diet. No change in blood cell counts was found after either diets (Figure S3). These results show the induction of a rapid systemic inflammatory response after HFD but not after SD consumption.

HFD induces a postprandial endotoxemic response.

Nutritional obesity is associated with increased blood levels of lipopolysaccharide (LPS), a constituent of Gram-negative bacteria (78). This bacterial component acts on peripheral metabolism and might also affect food intake (16,28). Thus, we examined blood levels of LPS in SD- and HFD-fed mice. We found that consumption of SD for 1 hour did not alter levels of circulating LPS (Figure 7A). However, consumption of HFD significantly increased levels of LPS in the blood as soon as 40 minutes after food introduction.

LPS enters systemic circulation via a transcellular pathway during fat absorption and can also translocate from the gut lumen to blood vessels via a paracellular pathway once the gut barrier is altered. We evaluated intestinal paracellular permeability in mice after 1h-SD and 1h-HFD by measuring fluorescein sodium salt (FSS) diffusion through gut biopsies mounted in Ussing chambers. We found higher permeability in the jejunum from 1h-HFD mice compared to 1h-SD (Figure 7B). These results indicate impaired gut permeability and endotoxemia at the time scale of a meal after HFD but not SD consumption.

Antibiotic-induced microbiota depletion affects postprandial metabolic responses but does not inhibit postprandial GLP-1, inflammatory or endotoxemic responses.

ABX treatment affected feeding behavior only under HFD. Therefore, we evaluated the effects of ABX treatment on different biological outcome parameters affected by 1h-HFD. We compared 1h-HFD and preprandial (control) mice that received or did not receive ABX treatment. We first examined the effect of ABX treatment on levels of cecal SCFA, which were analyzed by gas chromatography. Although the amount of cecal SCFA was substantial in ceca from untreated mice, these contents became undetectable in 1h-HFD ABX-treated mice (Figure 8A), indicating that microbiota metabolism was dramatically reduced by the ABX treatment.

Cecal biochemical assays were completed by ^1H NMR-based metabolomic analysis of plasma samples from the same mice. Statistical orthogonal projection on latent structure-discriminant analysis (O-PLS-DA) revealed a specific metabolic profile in plasma from 1h-HFD mice as compared to preprandial mice (Figure 8B). Conversely, the global analysis indicated no significant difference between samples from untreated and ABX-treated 1h-HFD mice. Interestingly, of all the identified NMR spectra, trimethylamine, a molecule produced by the gut microbiota, was the only circulating metabolite found to be affected by ABX. In fact, postprandial plasma levels of trimethylamine were significantly increased in 1h-HFD fed mice, but ABX treatment completely prevented this HFD-induced postprandial rise (Figure 8C).

We subsequently examined the effect of ABX treatment on the postprandial GLP-1 response. Again, plasma levels of total GLP-1 were elevated in 1h-HFD mice compared to

those of preprandial mice (Figure 8D). Remarkably, plasma levels of total GLP-1 were further increased in samples from ABX-treated mice under HFD for 1 hour.

To investigate the influence of the microbiota on the HFD-induced postprandial inflammatory response, we analyzed expression of pro-inflammatory markers in jejunum tissues. As observed before, expression levels of IL-1 β , TNF α , and COX-2 mRNAs were increased in 1h-HFD mice relative to preprandial mice (Figure 8E). Interestingly, ABX treatment did not alter postprandial induction. In addition, expression levels of NRF2, CAT, and SOD in the jejunum remained unchanged in 1h-HFD samples and were unaffected by the ABX treatment (Figure 8F).

Finally, we analyzed the HFD-induced postprandial endotoxemic response in microbiota-depleted mice. The level of circulating LPS was increased in plasma samples from 1h-HFD mice, and this HFD-induced endotoxemic response was not affected by the ABX treatment (Figure 8G).

The NLRP3-inflammasome is not involved in the short-term regulation of food intake.

The postprandial release of IL-1 β regulates metabolism and behavior (30,61). Maturation of pro-IL-1 β into its active and secreted form usually requires the proteolytic activity of caspase-1, which is under the control of a multi-protein complex, the inflammasome (79). ASC (Apoptosis-associated Speck-like protein containing a CARD) and NLRP3 (NOD-, LRR- and Pyrin domain-containing 3), two components of inflammasome, are both involved in the outcome of metabolic disorders (80). To determine the role of ASC and NLRP3 in the short-term regulation of food intake, we examined the feeding behavior of genetically modified mice lacking ASC or NLRP3 (ASC-KO and NLRP3-KO mice, respectively). Deficient mice were exposed to either SD or HFD for 1 hour, and compared to wild-type (WT) mice. The feeding behavior of ASC-KO mice was similar to that of WT mice, regardless of the diet (Figure 9A-B). Similar results were found in NLRP3-KO mice (Figure 9C-D). At the time of testing, ASC-KO mice had significantly lower body weight compared to controls and there were no significant differences in body weight for NLRP3-KO mice versus controls (Figure S4).

Since compensatory mechanisms that are inherent to genetic models might have masked the role of ASC and NLRP3 in the short-term regulation of feeding behavior, we performed a pharmacological experiment in adult WT mice using MCC950, a small-molecule inhibitor of the NLRP3-inflammasome (25). Treated mice received an intraperitoneal injection of MCC950 (20 mg/kg) 2 hours before the test. Control mice received vehicle (saline). As per the experiments described above, mice were fed either a SD or a HFD for 1 hour. MCC950 did not alter feeding behavior in mice under SD or HFD (Figure 9E-F). Taken together, these experiments suggest that the NLRP3-inflammasome is not involved in the short-term regulation of food intake.

LPS-binding toll-like receptor 4 (TLR4) receptor is not involved in the short-term regulation of food intake

In the host, LPS is sensed by the pattern-recognition TLR4 receptor (45). To address the role of TLR4 in the short-term control of food intake, we used mice deficient in TLR4 (TLR4-KO mice). We compared feeding behavior in TLR4-KO and WT mice. As described above, behavior was analyzed with either SD or HFD for 1 hour. The feeding behavior of TLR4-KO mice was not different from that of WT mice, regardless of the diet (Figure 9G-H).

We performed an additional pharmacological experiment in adult WT mice using TAK-242, a TLR4 antagonist (83). Mice received either an intraperitoneal injection of TAK-242 (10 mg/kg) or vehicle (saline), 2 hours before the behavioral test. TAK-242 did not alter feeding behavior in mice in response to SD or HFD for 1 hour (Figure 9I-J). Taken together, these results suggest that TLR4 is not involved in the short-term regulation of food intake.

Discussion

In this study, we provide evidence for the constitutive microbial control of food intake at the time scale of a meal in mice. We found that food intake was abnormally increased in microbiota-depleted mice after a high-fat meal, showing that the microbiota is able to regulate food intake under normal physiology, i.e., in healthy mice, with no need of additional microbiota boosters. This result is consistent with current theories supporting a beneficial effect of the microbiota on appetite regulation (2,34,54,89).

Importantly, the behavioral effect of the microbiota appeared after a high-fat meal only and was not observed after a balanced meal, showing that an interaction between food and the microbiota elicits the anorectic effect. Similar results have been found in overfed mice kept on HFD for 3 days, for which excessive calorie consumption was aggravated by microbiota depletion (56). Likewise, no microbiota-dependent anorectic effect has been established in control mice maintained on SD (56,92). Thus, these data reveal the constitutive and macronutrient-dependent anorectic effect of the gut microbiota.

Characterization of the constitutive microbial effect on feeding behavior

We found that the number of feeding bouts increased and the time between bouts decreased in microbiota-depleted mice fed HFD, suggesting that microbial activity under the HFD increases inter-bout intervals and that microbiota-derived factors are satietogenic. The positive effect of the microbiota on satiety has been already proposed, but most studies (i) found that the microbiota altered host satiety-related signaling and brain pathways without evidence for a functional outcome, and/or (ii) reported an effect on cumulative food intake but not on the structure of feeding behavior (12,33,74,85). Other preclinical studies have addressed the anorectic role of microbiota specifically during obesity or diabetes (4,20,36). In the few behavioral studies showing an effect of the microbiota on satiety, the microbiota was stimulated experimentally with pre- or probiotics prior to analyses, or isolated bacterial molecules were given before a feeding test (5,11,17,18,21,76). In this study, we demonstrate that constitutive microbes can contribute to satiety in normal physiological conditions after consumption of a high-fat meal.

Seeking the satietogenic pathway that mediates the anorectic effect of microbiota during HFD consumption

How could the gut microbiota influence satiety under physiological conditions? Details of this relationship are not completely understood. In this study, we explore the contribution of four well-known microbiota-associated routes in the gut-brain axis including metabolic, hormonal, immune and endotoxemic pathways.

We found that the satiety effect of the microbiota occurred after a high-fat meal only, with the postprandial inflammatory response. In particular, our data indicate reduced

immune cell infiltration in intestinal tissues under HFD, which could lower local immunity and increase susceptibility to pathogens. A shift in gut immune cell populations has been already reported in response to HFD for a few days, likely reflecting cell migration toward the peritoneal cavity, adipose tissues and liver (30,38,49,62). Here, we show that gut immune cell remodeling is induced very rapidly after HFD consumption. Thus, this process might contribute to the postprandial inflammatory response. Although induction of postprandial inflammatory reactions by a high-fat meal has been already reported (22,42,43,65), the physiological role of this response remains unclear. Recently, the postprandial release of IL-1 β was found to be required for the accurate homeostatic control of peripheral glucose metabolism (30). Moreover, IL-1 β signaling is involved in the initiation of postprandial fatigue, suggesting that the postprandial surge of this cytokine might act centrally (61). Nevertheless, behavioral studies from our genetic and pharmacological models, including ASC-KO, NLRP3-KO, and MCC950-treated mice, show that inhibition of the NLRP3-inflammasome, a master regulator of inflammatory responses, does not alter HFD feeding during the first hour, suggesting that postprandial inflammation does not contribute to the regulation of food intake within 1 hour of HFD. Interestingly, the commensal gut microbiota composition remains unchanged in inflammasome-deficient mice, which minimizes confounding factors (66). In addition, molecular studies show that HFD-induced intestinal inflammatory markers were not suppressed by the ABX treatment. This is in line with a previous study showing that the postprandial rise in circulating IL-1 β is not affected by microbiota depletion (30). Thus, ABX-insensitive postprandial inflammatory responses are probably not involved in the HFD-dependent anorectic effect of microbiota. Although the present study does not support a role for the postprandial NLRP3-mediated inflammatory response in feeding behavior within 1 hour, possible roles for other inflammatory pathways in feeding behavior should not be totally excluded. More delayed effects of the gradual inflammatory response should be also examined. Indeed, disruption of the NF- κ B signaling in the brain impairs the homeostatic feeding response to dietary fat (13).

We also found that ABX did not change basal expression of key redox markers in the gut. Moreover, levels of redox markers in the jejunum were not affected by either HFD

or ABX. These data suggest that the postprandial microbiota-dependent regulation of food intake during HFD does not engage marked changes in the intracellular redox state in the gut.

Consistent with previous rodent and human studies, we described a specific postprandial endotoxemic response to HFD (22,32,59,90). Interestingly, the level of circulating LPS is positively correlated with energy intake and sustained endotoxemia might deregulate food intake (3,28). However, in our study, HFD-induced postprandial endotoxemia was not reduced by the ABX treatment while food intake increased. The remaining systemic LPS in microbiota-depleted mice fed with a HFD for 1 hour might be derived from ingested foods, as was previously proposed to explain detection of basal levels of blood LPS in germ-free animals (15). LPS might reach the blood compartment more easily when dietary fats are consumed and/or when gut permeability is altered. Thus, short-term control of food intake after a high-fat meal does not seem to depend on circulating LPS, which has a well-established anorectic effect. Indeed, genetic and pharmacological interventions targeting TLR4, the mammalian endotoxin sensor, failed to inhibit food intake under HFD, indicating that TLR4 signaling is not involved in the control of food intake at the time scale of a meal. Interestingly, the postprandial inflammatory response does not require TLR4 activation either (43). Although LPS alters peripheral metabolism during sustained HFD exposure and might influence long-term regulation of food intake, the functional effect of the early postprandial rise of blood LPS remains to be elucidated, and the role of additional LPS sensors should be considered in this case (68).

To investigate whether the hormonal route could mediate the microbiota-derived satietogenic effect in our model, we examined the postprandial GLP-1 response as a relevant marker. We observed an elevated level of total GLP-1 in plasma of mice fed a HFD for 1 hour. Remarkably, ABX did not reduce this hormonal response in 1h-HFD mice but further increased it. This result is consistent with previous studies suggesting that the microbial metabolism negatively regulates GLP-1 levels (91). At the same time, abnormal elevated food intake was found in HFD-fed ABX-treated mice. Thus, the elevated plasma levels of total GLP-1 in ABX-treated mice corroborates the ABX-induced hyperphagia under HFD and can be viewed as a physiological consequence of the excessive feeding without an

immediate behavioral effect. Since GLP-1 is anorectic (14,84), these data show that during the 1h-HFD test, the microbiota does not modulate feeding behavior via the GLP-1 signaling pathway. If GLP1-sensitivity is maintained in ABX-treated mice, delayed GLP-1 action would probably take place after the 1-hour test period.

Finally, the roles of hormonal, immune and endotoxemic pathways in the mediation of the microbiota-derived anorectic effect during a high fat meal appear unlikely. More studies are needed to identify pathways and mediators underlying this effect. Nevertheless, we observed that the microbiota-derived anorectic effect happens under HFD only, a nutritional condition characterized by a specific microbial metabolic signature detectable both in the gut and in the blood. Indeed, we found a brief elevation of cecal branched SCFA after 20 minutes of HFD consumption. Cecal acetate, propionate, butyrate and valerate also increased under HFD at this time point, but did not reach statistical significance. Branched SCFA, such as isovalerate and isobutyrate, are end-products of bacterial proteolytic fermentation (64). The production of branched SCFA increases during acute consumption of animal-based food (27). Although some studies reported an effect of branched SCFA on gut motility, colonocyte functions, and liver metabolism, the impact of these molecules on the host feeding behavior is still unknown (10,41,48). The proton NMR-based metabolomic analysis failed to discriminate a global ABX-sensitive postprandial metabolic response in the blood after HFD consumption, however it is clear that the HFD-induced postprandial increase in blood trimethylamine was lessened by the ABX treatment. This result shows that some microbial molecules can reach the systemic compartment in response to the type of ingested food. Thus, microbial metabolites produced in the gut lumen could have initiated a HFD-specific behavioral response either locally in the gut or directly in brain centers via the humoral route. Further analyses in the proximal intestine and over shorter postprandial periods will help to better delineate all these metabolic changes. Likewise, more precise assays, for instance using liquid chromatography/mass spectrometry to measure microbial molecules in arterial and portal blood are required to obtain a comprehensive view of postprandial changes in these metabolites. It would also be interesting to investigate the role of trimethylamine in the control of feeding behavior. Other bacterial enterosynes, including microbiota-derived neurotransmitters, gaseous active molecules, aromatic compounds, and mimetics, which are known to modulate host

metabolism and behavior, should be also investigated in the future (1,34,55). The gut endocannabinoid system could be involved as well since related bioactive lipids can mediate the effects of the gut microbiota on host metabolism (70). Most of these molecular actors can be sensed locally by the enteric nervous system to modulate the brain postprandial response (19).

Methodological considerations

One limitation of our study is that we did not include prandial drinking in the meal definition although “drinking-explicit” models are proposed to be the most appropriate methods for analyzing meal patterns (81,93). Thus, the measurement of feeding bouts alone does not fully reflect the entire ingestive behavior and might provide an approximation of meal structure. Second, we analyzed raw feeding bouts without any mathematical corrections. Re-analyzing data in meals using a standard 5-minute inter-meal interval provided similar results (Figure S5). The size and duration of meals tended to increase in HFD-fed mice treated with antibiotics, suggesting that microbiota could be also involved in satiation. Indeed, we found increased cumulative food intake and increased time of feeding bouts and meals within the first hour of HFD in microbiota-depleted mice. Thus, regardless of the model used for assessing feeding behavior, these results indicate that the microbiota modulates the short-term regulation of food intake under physiological conditions.

Based on the antibiotic-induced microbiota depletion approach, we found evidence for the contribution of the microbiota in the feeding behavior in adult mice. In contrast, we failed to reproduce a similar phenotype in germ-free (GF) mice. Indeed, GF mice did not eat more than conventional (conv) mice during 1h-HFD (Figure S6), despite careful matching in age and weight of GF and conv mice during the experiment. For the antibiotic depletion, we used a typical mix of drugs including ampicillin, neomycin sulfate, metronidazole, and vancomycin. Anatomical, molecular, biochemical and bacteriological analyzes of cecum content and feces indicated that our protocol strongly depleted gut bacteria. Despite this, the presence of some antibiotic-resistant bacteria living after the pharmacological intervention was still probable. However, unlike in germ-free mice in which the absence of microbes is complete and constant over the lifespan, the use of antibiotics avoids critical defects in immune and homeostatic systems observed in adult GF mice (51). Thus, one can

speculate that defects in GF mice might have altered the microbiota-derived satietogenic effect that happens in conventional mice.

In our study, the antibiotic dosage was increased progressively to acclimate the mice to the bitter taste and to ensure normal hydration. Treatment was not supplemented with sweeteners or antifungals. It was designed first and foremost to maintain normal metabolism and behavior prior to the feeding test. Indeed, the body weight and feeding behavior of ABX-treated mice were unchanged under SD using this protocol. Nevertheless, we found that the treatment increased food intake when fatty foods were consumed, highlighting the role of microbiota in the control of food intake. Since the gut microbiota influences various satiety-related pathways, the effect of the treatment was likely derived from gut microbiota depletion. On the other hand, commensal bacteria reside in various parts of the body, including the mouth, and recent studies suggest a link between the oral microbiota and food preference (23,31,67). Similar studies established a link between olfactory microbiota and olfactory epithelium functioning (35,71). Accordingly, a change in taste and smell perception might account for the increase in food intake in HFD-fed mice under antibiotic treatment. However, we found that the size and duration of feeding bouts were not changed in microbiota-depleted mice, which is not in favor of an alteration in olfacto-gustatory sensing, in food preference and satiation.

Conclusion

This work provides evidence that commensal bacteria promote satiety in mice under healthy conditions. We found that the microbial anorectic effect develops according to the composition of the meal. Strikingly, the microbiota limits excessive calorie consumption in mice eating high-fat food, highlighting the homeostatic role of the microbiota over the course of normal physiology. This finding strengthens the concept that appetite is shaped by complex interactions between diet and commensal bacteria.

Materials and Methods

Electronic laboratory notebooks were not used.

Animals

All protocols involving animals were reviewed and approved by the local ethics committee and were in strict accordance with the European Community guidelines. All protocols were agreed by the French Ministry of Higher Education, Research and Innovation (accreditation no. APAFIS#18117 and #1285-2015102618593445v3). Most experiments were carried out on 7/9-week-old male C57Bl/6J mice from Charles River Laboratory (France). We also examined transgenic homozygous *Asc*^{-/-}, *Nlrp3*^{-/-} and *Tlr4*^{-/-} mice (named hereinafter ASC-KO, NLRP3-KO and TLR4-KO mice, respectively), which were bred in a C57Bl/6J genetic background. Transgenic animals were compared to wild-type mice bred in the same environment. All animals were housed at 22.5 ± 1°C on a 12h-12h reversed light-dark cycle (light off at 10:30 a.m.; light on at 10:30 p.m.), in a specific pathogen-free facility. Before experiments, mice had free access to food and water.

For the study on germ-free (GF) and conventional (conv) mice, GF mice were obtained from Anaxem germ-free animal facilities of the Micalis Institute, INRAE (France), and conv mice were purchased from Charles River Laboratory (France). Mice were 8-week-old C57Bl/6J males. GF and conv mice were transferred to two separated sterile isolators (Eurobioconcept, France) allowing the continuous maintenance of sterility as described previously (69). Inside the isolators, the animals were housed in individual cages containing sterile bedding and had free access to autoclaved tap water and γ-irradiated (45 kGy) food. The animal room was maintained at 22 ± 2°C and kept on a 12h light/dark cycle (lights on at 7:30 a.m.).

Antibiotic treatment

At the beginning of the treatment, animals were housed individually. Antibiotics were provided in drinking water for 15 days. The mix contained ampicillin (1 g/l; cat. no. A-9518; Sigma-Aldrich), neomycin sulfate (1 g/l; cat. no. N1876; Sigma-Aldrich), metronidazole (1 g/l; cat. no. M3761; Sigma-Aldrich) and vancomycin (0.5 g/l; cat. no. 00315; Chem Impex International). Drugs were diluted in a final volume of 15 ml. The dosage was increased gradually (1/100, 1/30, 1/10, 1/3, 1) to reach final concentration after 4 days (Figure 1A). Antibiotics were changed every day for the first 4 days, and then renewed every second day.

Experimental design

For experiments, mice were single-caged and food was removed for 2 hours before lights off as previously described (73) (Figure S1C). Mice were trained to the food removal three times. Preprandial mice were sacrificed at the end of the food restriction period, at 10:30 a.m. Postprandial mice received food at the beginning of the dark period and were sacrificed at different time points (i.e., 20, 40 and 60 minutes) after food introduction. During the tests, food was either the standard diet (SD; cat. no. A04; SAFE) or a semi-synthesized high-fat diet (HFD; cat. no. U8954 v7; SAFE) (Figure S1D). To prevent food neophobia, mice received one HFD pellet for 10 minutes one day before trial. For axenic experiments, food was γ -irradiated (45 kGy) SD or HFD. Before sacrifice and dissection, mice were anesthetized by intraperitoneal injection of a ketamine-xylazine mix (120-24 mg/kg).

Drug administration

TAK-242, a TLR4 antagonist (cat. no. R-3152492-1; Merck), was prepared in 0.9% NaCl containing 1% DMSO. MCC950, a NLRP3-inflammasome inhibitor (cat. no. HY-12815A; CliniSciences), was prepared in PBS. Dosage was 10 mg/kg TAK-242 and 20 mg/kg MCC950, injected intraperitoneally (100 μ l), 2 hours before lights off, according to previous pharmacokinetic/pharmacodynamic studies (24,25,46). Controls received saline. Before experiments, mice were trained 3 times with ip injections of saline once a day before lights off. For experiments, mice were randomly assigned to receive TAK-242, MCC950 or vehicle.

Feeding behavior analysis

Except in axenic experiments, food intake was recorded using the BioDAQ System (Research Diets, USA). Mice were acclimatized for 3 days to single housing and feeding through the food hopper. Cages contained enrichment and bedding material. Water was given *ad libitum* from regular bottles placed on the top of the cage. During habituation and experiments, food hoppers were closed for 2 hours before lights off. Data were collected continuously and were analyzed using the BioDAQ DataViewer software (Research Diets, USA). For the analysis, the minimum food amount was filtered at 0.02 g and minimum inter-bout interval was set at 5 s. For the axenic experiment, food intake was measured manually.

Blood biochemistry

Mice were anesthetized and blood was collected by cardiac puncture in EDTA-coated tubes. Aliquots were sent to the CerbaVet laboratory for complete blood count (Wissous, France). Plasma samples were obtained by centrifugation at 2650 *g* for 10 min at 7°C. Plasma levels of total GLP1 were measured by ELISA using the Total GLP-1 NL-ELISA kit (cat. Number 10-1278-01; Mercodia). Plasma levels of cytokines were measured using a V-Plex multiplex assay (Meso Scale Discovery, USA), according to the manufacturer's protocol. The plasma LPS concentration was determined by direct quantitation of 3-hydroxymyristate (or 3HM) by HPLC/MS/MS as previously described (75). An initial HCl hydrolysis step was conducted to distinguish between unesterified 3HM and esterified 3HM, i.e., true LPS. Thus, the LPS concentration was defined as total 3HM (as assessed after HCl hydrolysis) minus unesterified 3HM concentration (as assessed without HCl hydrolysis).

Quantitative assay of the bacterial 16S rRNA gene

The analysis was performed on fresh feces, which were first snap-frozen and stored at -80°C. The DNA extraction and assay were performed by the Biomnigene company. Samples were lysed and extracted using the E.Z.N.A DNA Stool kit (Omega Bio-tek). Extracted DNA was quantified using a Qubit 4 Fluorometer (ThermoFisher). Quantitative PCR targeting the 16S rRNA gene was performed using PowerUp™ SYBR™ Green Master Mix (Applied Biosystems), with the following primers: Forward 5' CCT ACG GGA GGC AGC AG 3', reverse, 5' ATT ACC GCG GCT GCT GGC A 3'. A dilution series (from 0.0064 ng to 100 ng) of a sample derived-plasmid construct containing the target amplicon was run in parallel for absolute quantification. Reactions were performed on a QuantStudio 3 thermocycler (Applied Biosystems), with the following PCR cycling conditions: 50°C for 2 min, 95°C for 15 min followed by 35 cycles including 95°C for 15 s, 60°C for 30 s, and 72°C for 30 s, followed by a step at 80°C for 20 s and a final step for melt curve analysis.

Fecal cultures

Fresh feces were collected in sterile tubes and mixed with PBS (1 g/ml feces/PBS). Feces were emulsified by vigorous vortex agitation for 5 minutes, 500 µl of supernatant was

spread on plates containing solid sterile LB agar. Plates were incubated under aerobic conditions for 3 days at 37°C.

Cecal SCFA assay

Cecal samples were water-extracted and proteins were precipitated with phosphotungstic acid as described previously (57). For the assay, 0.3 µl of the supernatant together with 2-ethylbutyrate as an internal standard were injected into a gas-liquid chromatograph (Agilent 6890, France), which was equipped with a split-splitless injector 7850, a flame ionization detector and a capillary polyethylene glycol column (15 m, 0.53 mm, 0.5 µm). The flow rate of the carrier gas (He) non H₂ was 10 ml/min. Inlet, column and detector temperatures were 200, 100 and 240°C, respectively. The column temperature was first set at 100°C, held for 15 min, then programmed from 100 to 180°C at a rate of 20°C/min and held 2 min. 2-Ethylbutyrate was used as an internal standard. Data were collected and peaks integrated with openLab software, CDS GC ChemStation (Agilent, les Ulis, France)

Proton Nuclear Magnetic Resonance (¹H-NMR)-based metabolomics

Plasma samples were prepared for NMR analysis as described previously (8). All ¹H-NMR spectra were obtained on a Bruker DRX-600-Avance NMR spectrometer (Bruker) using the AXIOM metabolomics platform (MetaToul) operating at 600:13MHz for ¹H resonance frequency. Data acquisition, pretreatment and statistical analysis were performed as described previously (63). Areas under the curve of several signals of interest were integrated and significance tested with a Mann-Whitney test.

Gene expression assay in gut biopsies

Mice were anesthetized and fragments of duodenum, jejunum, ileum and colon were collected, snap-frozen and stored at -80°C until use. Total RNAs were extracted using RNeasy Plus Mini Kit (Qiagen), according to the manufacturer's protocol. Briefly, tissues were disrupted using lysis buffer and a TissueLyser (Qiagen). Lysates were first spun through gDNA Eliminator spin columns to remove genomic DNA. Total RNA was then purified using RNeasy Mini spin columns. The concentration and integrity of extracts were assessed by spectrophotometry (Nanodrop 2000; ThermoFischer Scientific) and with the Experion automated electrophoresis system (Bio-Rad). Reverse transcription was performed on 500

ng of total RNA using SuperScript IV VILO Master Mix (ThermoFischer). PCRs were carried out in a 10 µl reaction volume containing 2 µl of 1:5 diluted cDNA, 2 µl of nuclease-free water, 5 µl of Taqman fast advanced Master Mix (Applied Biosystems), and 1 µl of appropriate Taqman probes (Applied Biosystems) for POLR2A (Mm00839502), IL-1β (Mm00434228), TNFα (Mm00443258), COX-2 (Mm00478374), NRF2 (Mm00 477784_m1), CAT (Mm00 437992_m1), and SOD (Mm0 1344233_g1). Real-time PCRs were run on a StepOnePlus thermocycler (Applied Biosystems). The comparative CT method was used for relative quantification (RQ) of target genes, using POLR2A as a reference gene and the preprandial condition as a control.

Analysis of gut permeability

Mice were anesthetized and intestinal tissues were removed and opened longitudinally. Desired intestinal sections were cut and mounted in an Ussing chamber system (Physiologic Instrument, San Diego, USA). The chamber opening exposed 0.5 cm² of tissue surface area to oxygenated buffered solutions at 37°C. The serosal chamber was filled with 10 mM glucose-Krebs solution to provide fuel to the tissue, and the mucosal chamber was filled with 10 mM mannitol-Krebs solution to maintain osmotic balance. Paracellular permeability was determined using Fluorescein Sodium Salt (FSS; 0.38 kDa), which was added to the mucosal chamber at t0. Medium from serosal chambers was sampled every 30 minutes for 120 minutes. The concentration of FSS was measured by fluorimetry at an excitation wavelength of 485 nm and an emission wavelength of 535 nm.

Immunostaining in histological gut sections

Mice were anesthetized, intestines were dissected and intestinal segments were selected. Collected tissues were fixed overnight in 4% paraformaldehyde before embedding in paraffin. Paraffin-embedded tissues were cut and sections were deparaffinized and rehydrated. Endogenous peroxidases were quenched with 3% hydrogen peroxide. Nonspecific binding of antibodies was prevented with 3% BSA. Sections were incubated with primary antibodies diluted with 1% BSA in PBS, overnight at 4°C. After washing, sections were incubated with a HRP-conjugated secondary antibody for 30 minutes at room temperature. Immune complexes were detected with NovaRed peroxidase substrate (cat. no. #SK4800; Vector Labs). Sections were counterstained with Harris hematoxylin, washed

and mounted. Immunolabeling was analyzed using ImageJ software, using the Color Deconvolution and Statistical Region Merging parameters.

Primary antibodies were: rat anti-mouse F4/80 for detection of macrophages (dilution: 1/100, cat. no. MCA497; AbD Serotec); rabbit anti-CD4 for detection of T-helper lymphocytes (dilution: 1/1000; cat. no. ab1836858; Abcam); and rabbit anti-CD8 for detection of cytotoxic T lymphocytes (dilution: 1/1000, cat. no. ab217344; Abcam). Secondary antibodies were: anti-rat IgG (cat. no. #MP-7404; Vector Labs) for F4/80-positive cells; and anti-rabbit IgG (cat. no. #MP-7401; Vector Labs) for CD4-positive and CD8-positive cells.

Statistics

Statistical analyses were performed using Prism 5.0 software (GraphPad Software, Inc.). No statistical method was used to predefine sample size. Results on graphs were expressed as boxplot with individual data from min and max. Multiple comparisons of groups were carried out using one-way analysis of variance (ANOVA) followed by a post hoc Newman-Keuls test. Equality of variances and normality of distribution were checked prior each analysis. The Mann-Whitney test was used for 2 group comparison and for nonparametric multiple comparisons. No correction was applied on data for analysis. A p value <0.05 was considered statistically significant.

Acknowledgments

We thank the animal facility of the CSGA, especially Anne Lefranc, Martin Bertomeu, and Virginie Cadiou for animal care, the CellImaP imaging facility of the Université de Bourgogne, especially André Bouchot, and Audrey Geissler for histological studies, and the Lipidomic facility of the Université de Bourgogne, especially Jean-Paul Pais de Barros for LPS assay. We thank the Biomnigene Company and especially Alexandre Douablin for 16S RNA gene analyses. We thank students who assisted researchers, especially Alice Crétin-Anciaux, Sophie Lahmar, Marie Janod, and Laura Guénot. We thank Vishva Dixit (Genentech) for providing ASC^{-/-} mice and the ANIRA-PBES animal facility of SFR Biosciences (UAR3444/CNRS, US8/Inserm, ENS de Lyon, UCBL), for breeding these mice. We thank Abby Cuttriss (Office of International Scientific visibility) for editing the manuscript.

This work was supported by the French “Investissements d’Avenir” program, project ISITE-BFC (contract ANR-15-IDEX-0003), by the ANR (contract ANR-21-CE14-0033), by the Région Bourgogne and FEDER program (contract 2019-6200FEO047S00409) to AB; by the INRAE grant “Action Prioritaire du Département Alimentation Humaine” to AB, GB, and VD; by the Medisite Foundation and the French government, managed by the National Research Agency (ANR), through the UCAJEDI Investments in the Future project (contract ANR-15-IDEX-01) to CC, CS, JLN, and CR; by the LABEX SIGNALIFE program (contract ANR-11-LABX-0028-01) to JLN and CR; and by the Fondation pour la Recherche Médicale (contract DEQ20170336744) to VP.

Abbreviations used

ABX	antibiotic
ASC	apoptosis-associated speck-like protein containing a CARD
BSA	bovine serum albumin
CAT	catalase
CCL2, 5	C-C motif chemokine ligand-2, -5
CD4, CD8	cluster of differentiation 4, 8
ClpB	caseinolytic protease B
Conv	conventional
COX-2	cyclooxygenase-2
CT	cycle threshold
EDTA	ethylenediaminetetraacetic acid
ELISA	enzyme-linked immunosorbent assay
FSS	fluorescent sodium salt
GF	germ-free

GLP-1	glucagon-like peptide-1;
HFD	high-fat diet
HPLC/MS/MS	high-performance liquid chromatography coupled with tandem mass spectrometry
HRP	horseradish peroxidase enzyme
IFN γ	interferon γ
IgG	immunoglobulin G
IL-1 β , -6, -10	interleukin-1 β , -6, -10
LB	lysogeny broth
LPS	lipopolysaccharide
MCP1	monocyte chemoattractant protein-1
NF- κ B	nuclear factor-kappa B
NLRP3	NOD-, LRR- and Pyrin domain-containing 3
NRF2	nuclear factor erythroid 2-related factor 2
O-PLS-DA	orthogonal projection on latent structure-discriminant analysis
PBS	phosphate-buffered saline
PCR, qPCR	polymerase chain reaction; quantitative PCR
POLR2A	RNA polymerase II subunit A
POMC	pro-opiomelanocortin
RANTES	regulated upon activation, normal T-cell expressed and secreted
RQ	relative quantification
RT-qPCR	reverse transcription-quantitative PCR

SCFA	short chain fatty acid
SD	standard diet
SOD	superoxide dismutase
T cell	Thymus derived lymphocyte
TLR4	toll-like receptor
TNF α	tumor necrosis factor α
WT	wild-type
α -MSH	α -melanocyte-stimulating hormone
1H-NMR	proton nuclear magnetic resonance based metabolomics analysis
3HM	3-hydroxymyristate

References

1. Abot A, Wemelle E, Laurens C, Paquot A, Pomie N, Carper D, Bessac A, Mas Orea X, Fremez C, Fontanie M, Lucas A, Lesage J, Everard A, Meunier E, Dietrich G, Muccioli GG, Moro C, Cani PD, Knauf C. Identification of new enterosynes using prebiotics: roles of bioactive lipids and mu-opioid receptor signalling in humans and mice. *Gut*, 2020.
2. Alcock J, Maley CC, Aktipis CA. Is eating behavior manipulated by the gastrointestinal microbiota? Evolutionary pressures and potential mechanisms. *Bioessays* 36: 940-9, 2014.
3. Amar J, Burcelin R, Ruidavets JB, Cani PD, Fauvel J, Alessi MC, Chamontin B, Ferrieres J. Energy intake is associated with endotoxemia in apparently healthy men. *Am J Clin Nutr* 87: 1219-23, 2008.
4. Anastasovska J, Arora T, Sanchez Canon GJ, Parkinson JR, Touhy K, Gibson GR, Nadkarni NA, So PW, Goldstone AP, Thomas EL, Hankir MK, Van Loo J, Modi N, Bell JD, Frost G. Fermentable carbohydrate alters hypothalamic neuronal activity and protects against the obesogenic environment. *Obesity (Silver Spring)* 20: 1016-23, 2012.
5. Archer BJ, Johnson SK, Devereux HM, Baxter AL. Effect of fat replacement by inulin or lupin-kernel fibre on sausage patty acceptability, post-meal perceptions of satiety and food intake in men. *Br J Nutr* 91: 591-9, 2004.
6. Astbury NM, Taylor MA, Macdonald IA. Polydextrose results in a dose-dependent reduction in ad libitum energy intake at a subsequent test meal. *Br J Nutr* 110: 934-42, 2013.
7. Bagarolli RA, Tobar N, Oliveira AG, Araujo TG, Carvalho BM, Rocha GZ, Vecina JF, Calisto K, Guadagnini D, Prada PO, Santos A, Saad STO, Saad MJA. Probiotics modulate gut microbiota and improve insulin sensitivity in DIO mice. *J Nutr Biochem* 50: 16-25, 2017.

8. Beckonert O, Keun HC, Ebbels TM, Bundy J, Holmes E, Lindon JC, Nicholson JK. Metabolic profiling, metabolomic and metabonomic procedures for NMR spectroscopy of urine, plasma, serum and tissue extracts. *Nat Protoc* 2: 2692-703, 2007.
9. Belkaid Y, Hand TW. Role of the microbiota in immunity and inflammation. *Cell* 157: 121-41, 2014.
10. Blakeney BA, Crowe MS, Mahavadi S, Murthy KS, Grider JR. Branched Short-Chain Fatty Acid Isovaleric Acid Causes Colonic Smooth Muscle Relaxation via cAMP/PKA Pathway. *Dig Dis Sci* 64: 1171-1181, 2019.
11. Breton J, Tennoune N, Lucas N, Francois M, Legrand R, Jacquemot J, Goichon A, Guerin C, Peltier J, Pestel-Caron M, Chan P, Vaudry D, do Rego JC, Lienard F, Penicaud L, Fioramonti X, Ebenezer IS, Hokfelt T, Dechelotte P, Fetissov SO. Gut Commensal *E. coli* Proteins Activate Host Satiety Pathways following Nutrient-Induced Bacterial Growth. *Cell Metab* 23: 324-34, 2016.
12. Brooks L, Viardot A, Tsakmaki A, Stolarczyk E, Howard JK, Cani PD, Everard A, Sleeth ML, Psichas A, Anastasovskaj J, Bell JD, Bell-Anderson K, Mackay CR, Ghatei MA, Bloom SR, Frost G, Bewick GA. Fermentable carbohydrate stimulates FFAR2-dependent colonic PYY cell expansion to increase satiety. *Mol Metab* 6: 48-60, 2017.
13. Buckman LB, Thompson MM, Lippert RN, Blackwell TS, Yull FE, Ellacott KL. Evidence for a novel functional role of astrocytes in the acute homeostatic response to high-fat diet intake in mice. *Mol Metab* 4: 58-63, 2015.
14. Burmeister MA, Ayala JE, Smouse H, Landivar-Rocha A, Brown JD, Drucker DJ, Stoffers DA, Sandoval DA, Seeley RJ, Ayala JE. The Hypothalamic Glucagon-Like Peptide 1 Receptor Is Sufficient but Not Necessary for the Regulation of Energy Balance and Glucose Homeostasis in Mice. *Diabetes* 66: 372-384, 2017.

15. Caesar R, Reigstad CS, Bäckhed HK, Reinhardt C, Ketonen M, Lundén G, Cani PD, Bäckhed F. Gut-derived lipopolysaccharide augments adipose macrophage accumulation but is not essential for impaired glucose or insulin tolerance in mice. *Gut* 61: 1701-7, 2012.
16. Cani PD, Amar J, Iglesias MA, Poggi M, Knauf C, Bastelica D, Neyrinck AM, Fava F, Tuohy KM, Chabo C, Waget A, Delmee E, Cousin B, Sulpice T, Chamontin B, Ferrieres J, Tanti JF, Gibson GR, Casteilla L, Delzenne NM, Alessi MC, Burcelin R. Metabolic endotoxemia initiates obesity and insulin resistance. *Diabetes* 56: 1761-72, 2007.
17. Cani PD, Dewever C, Delzenne NM. Inulin-type fructans modulate gastrointestinal peptides involved in appetite regulation (glucagon-like peptide-1 and ghrelin) in rats. *Br J Nutr* 92: 521-6, 2004.
18. Cani PD, Joly E, Horsmans Y, Delzenne NM. Oligofructose promotes satiety in healthy human: a pilot study. *Eur J Clin Nutr* 60: 567-72, 2006.
19. Cani PD, Knauf C. How gut microbes talk to organs: The role of endocrine and nervous routes. *Mol Metab* 5: 743-52, 2016.
20. Cani PD, Knauf C, Iglesias MA, Drucker DJ, Delzenne NM, Burcelin R. Improvement of glucose tolerance and hepatic insulin sensitivity by oligofructose requires a functional glucagon-like peptide 1 receptor. *Diabetes* 55: 1484-90, 2006.
21. Cani PD, Lecourt E, Dewulf EM, Sohet FM, Pachikian BD, Naslain D, De Backer F, Neyrinck AM, Delzenne NM. Gut microbiota fermentation of prebiotics increases satietogenic and incretin gut peptide production with consequences for appetite sensation and glucose response after a meal. *Am J Clin Nutr* 90: 1236-43, 2009.
22. Cansell C, Stobbe K, Sanchez C, Le Thuc O, Mosser CA, Ben-Fradj S, Leredde J, Lebeaupin C, Debayle D, Fleuriot L, Brau F, Devaux N, Benani A, Audinat E, Blondeau N, Nahon JL, Rovère C. Dietary fat exacerbates postprandial hypothalamic inflammation involving glial fibrillary acidic protein-positive cells and microglia in male mice. *Glia* 69: 42-60, 2021.

23. Cattaneo C, Riso P, Laureati M, Gargari G, Pagliarini E. Exploring Associations between Interindividual Differences in Taste Perception, Oral Microbiota Composition, and Reported Food Intake. *Nutrients* 11, 2019.
24. Chen W, Foo SS, Zaid A, Teng TS, Herrero LJ, Wolf S, Tharmarajah K, Vu LD, van Vreden C, Taylor A, Freitas JR, Li RW, Woodruff TM, Gordon R, Ojcius DM, Nakaya HI, Kanneganti TD, O'Neill LAJ, Robertson AAB, King NJ, Suhrbier A, Cooper MA, Ng LFP, Mahalingam S. Specific inhibition of NLRP3 in chikungunya disease reveals a role for inflammasomes in alphavirus-induced inflammation. *Nat Microbiol* 2: 1435-1445, 2017.
25. Coll RC, Robertson AA, Chae JJ, Higgins SC, Munoz-Planillo R, Inserra MC, Vetter I, Dungan LS, Monks BG, Stutz A, Croker DE, Butler MS, Haneklaus M, Sutton CE, Nunez G, Latz E, Kastner DL, Mills KH, Masters SL, Schroder K, Cooper MA, O'Neill LA. A small-molecule inhibitor of the NLRP3 inflammasome for the treatment of inflammatory diseases. *Nat Med* 21: 248-55, 2015.
26. Cryan JF, O'Riordan KJ, Cowan CSM, Sandhu KV, Bastiaanssen TFS, Boehme M, Codagnone MG, Cussotto S, Fulling C, Golubeva AV, Guzzetta KE, Jaggar M, Long-Smith CM, Lyte JM, Martin JA, Molinero-Perez A, Moloney G, Morelli E, Morillas E, O'Connor R, Cruz-Pereira JS, Peterson VL, Rea K, Ritz NL, Sherwin E, Spichak S, Teichman EM, van de Wouw M, Ventura-Silva AP, Wallace-Fitzsimons SE, Hyland N, Clarke G, Dinan TG. The Microbiota-Gut-Brain Axis. *Physiol Rev* 99: 1877-2013, 2019.
27. David LA, Maurice CF, Carmody RN, Gootenberg DB, Button JE, Wolfe BE, Ling AV, Devlin AS, Varma Y, Fischbach MA, Biddinger SB, Dutton RJ, Turnbaugh PJ. Diet rapidly and reproducibly alters the human gut microbiome. *Nature* 505: 559-63, 2014.
28. de La Serre CB, de Lartigue G, Raybould HE. Chronic exposure to low dose bacterial lipopolysaccharide inhibits leptin signaling in vagal afferent neurons. *Physiol Behav* 139: 188-94, 2015.

29. Delzenne NM, Cani PD, Daubioul C, Neyrinck AM. Impact of inulin and oligofructose on gastrointestinal peptides. *Br J Nutr* 93 Suppl 1: S157-61, 2005.
30. Dror E, Dalmas E, Meier DT, Wueest S, Thevenet J, Thienel C, Timper K, Nordmann TM, Traub S, Schulze F, Item F, Vallois D, Pattou F, Kerr-Conte J, Lavallard V, Berney T, Thorens B, Konrad D, Boni-Schnetzler M, Donath MY. Postprandial macrophage-derived IL-1 β stimulates insulin, and both synergistically promote glucose disposal and inflammation. *Nat Immunol* 18: 283-292, 2017.
31. Duca FA, Swartz TD, Sakar Y, Covasa M. Increased oral detection, but decreased intestinal signaling for fats in mice lacking gut microbiota. *PLoS One* 7: e39748, 2012.
32. Erridge C, Attina T, Spickett CM, Webb DJ. A high-fat meal induces low-grade endotoxemia: evidence of a novel mechanism of postprandial inflammation. *Am J Clin Nutr* 86: 1286-92, 2007.
33. Falcinelli S, Rodiles A, Unniappan S, Picchiatti S, Gioacchini G, Merrifield DL, Carnevali O. Probiotic treatment reduces appetite and glucose level in the zebrafish model. *Sci Rep* 6: 18061, 2016.
34. Fetissov SO. Role of the gut microbiota in host appetite control: bacterial growth to animal feeding behaviour. *Nat Rev Endocrinol* 13: 11-25, 2017.
35. François A, Grebert D, Rhimi M, Mariadassou M, Naudon L, Rabot S, Meunier N. Olfactory epithelium changes in germfree mice. *Sci Rep* 6: 24687, 2016.
36. Frost G, Sleeth ML, Sahuri-Arisoylu M, Lizarbe B, Cerdan S, Brody L, Anastasovska J, Ghourab S, Hankir M, Zhang S, Carling D, Swann JR, Gibson G, Viardot A, Morrison D, Louise Thomas E, Bell JD. The short-chain fatty acid acetate reduces appetite via a central homeostatic mechanism. *Nat Commun* 5: 3611, 2014.
37. Gakis G, Mueller MH, Hahn J, Glatzle J, Grundy D, Kreis ME. Neuronal activation in the nucleus of the solitary tract following jejunal lipopolysaccharide in the rat. *Auton Neurosci* 148: 63-8, 2009.

38. Garidou L, Pomie C, Klopp P, Waget A, Charpentier J, Aloulou M, Giry A, Serino M, Stenman L, Lahtinen S, Dray C, Iacovoni JS, Courtney M, Collet X, Amar J, Servant F, Lelouvier B, Valet P, Eberl G, Fazilleau N, Douin-Echinard V, Heymes C, Burcelin R. The Gut Microbiota Regulates Intestinal CD4 T Cells Expressing RORgammat and Controls Metabolic Disease. *Cell Metab* 22: 100-12, 2015.
39. Gee JM, Johnson IT. Dietary lactitol fermentation increases circulating peptide YY and glucagon-like peptide-1 in rats and humans. *Nutrition* 21: 1036-43, 2005.
40. Gribble FM, Reimann F. Function and mechanisms of enteroendocrine cells and gut hormones in metabolism. *Nat Rev Endocrinol* 15: 226-237, 2019.
41. Heimann E, Nyman M, Palbrink AK, Lindkvist-Petersson K, Degerman E. Branched short-chain fatty acids modulate glucose and lipid metabolism in primary adipocytes. *Adipocyte* 5: 359-368, 2016.
42. Herieka M, Erridge C. High-fat meal induced postprandial inflammation. *Mol Nutr Food Res* 58: 136-46, 2014.
43. Hermier D, Mathe V, Lan A, Santini C, Quignard-Boulange A, Huneau JF, Mariotti F. Postprandial low-grade inflammation does not specifically require TLR4 activation in the rat. *Nutr Metab (Lond)* 14: 65, 2017.
44. Honda K, Littman DR. The microbiota in adaptive immune homeostasis and disease. *Nature* 535: 75-84, 2016.
45. Hoshino K, Takeuchi O, Kawai T, Sanjo H, Ogawa T, Takeda Y, Takeda K, Akira S. Cutting edge: Toll-like receptor 4 (TLR4)-deficient mice are hyporesponsive to lipopolysaccharide: evidence for TLR4 as the Lps gene product. *J Immunol* 162: 3749-52, 1999.
46. Hua F, Tang H, Wang J, Prunty MC, Hua X, Sayeed I, Stein DG. TAK-242, an antagonist for Toll-like receptor 4, protects against acute cerebral ischemia/reperfusion injury in mice. *J Cereb Blood Flow Metab* 35: 536-42, 2015.

47. Hull S, Re R, Tiihonen K, Viscione L, Wickham M. Consuming polydextrose in a mid-morning snack increases acute satiety measurements and reduces subsequent energy intake at lunch in healthy human subjects. *Appetite* 59: 706-12, 2012.
48. Jaskiewicz J, Zhao Y, Hawes JW, Shimomura Y, Crabb DW, Harris RA. Catabolism of isobutyrate by colonocytes. *Arch Biochem Biophys* 327: 265-70, 1996.
49. Johnson AM, Costanzo A, Gareau MG, Armando AM, Quehenberger O, Jameson JM, Olefsky JM. High fat diet causes depletion of intestinal eosinophils associated with intestinal permeability. *PLoS One* 10: e0122195, 2015.
50. Kazemi A, Noorbala AA, Djafarian K. Effect of probiotic and prebiotic versus placebo on appetite in patients with major depressive disorder: post hoc analysis of a randomised clinical trial. *J Hum Nutr Diet* 33: 56-65, 2020.
51. Kennedy EA, King KY, Baldrige MT. Mouse Microbiota Models: Comparing Germ-Free Mice and Antibiotics Treatment as Tools for Modifying Gut Bacteria. *Front Physiol* 9: 1534, 2018.
52. Kim JS, de La Serre CB. Diet, gut microbiota composition and feeding behavior. *Physiol Behav* 192: 177-181, 2018.
53. King NA, Craig SA, Pepper T, Blundell JE. Evaluation of the independent and combined effects of xylitol and polydextrose consumed as a snack on hunger and energy intake over 10 d. *Br J Nutr* 93: 911-5, 2005.
54. Klingbeil E, de La Serre CB. Microbiota modulation by eating patterns and diet composition: impact on food intake. *Am J Physiol Regul Integr Comp Physiol* 315: R1254-R1260, 2018.
55. Knauf C, Abot A, Wemelle E, Cani PD. Targeting the Enteric Nervous System to Treat Metabolic Disorders? "Enterosynes" as Therapeutic Gut Factors. *Neuroendocrinology* 110: 139-146, 2020.

56. Krisko TI, Nicholls HT, Bare CJ, Holman CD, Putzel GG, Jansen RS, Sun N, Rhee KY, Banks AS, Cohen DE. Dissociation of Adaptive Thermogenesis from Glucose Homeostasis in Microbiome-Deficient Mice. *Cell Metab* 31: 592-604 e9, 2020.
57. Lan A, Bruneau A, Philippe C, Rochet V, Rouault A, Hervé C, Roland N, Rabot S, Jan G. Survival and metabolic activity of selected strains of *Propionibacterium freudenreichii* in the gastrointestinal tract of human microbiota-associated rats. *Br J Nutr* 97: 714-24, 2007.
58. Larraufie P, Martin-Gallausiaux C, Lapaque N, Dore J, Gribble FM, Reimann F, Blottiere HM. SCFAs strongly stimulate PYY production in human enteroendocrine cells. *Sci Rep* 8: 74, 2018.
59. Laugerette F, Vors C, Geloën A, Chauvin MA, Soulage C, Lambert-Porcheron S, Peretti N, Alligier M, Burcelin R, Laville M, Vidal H, Michalski MC. Emulsified lipids increase endotoxemia: possible role in early postprandial low-grade inflammation. *J Nutr Biochem* 22: 53-9, 2011.
60. Legrand R, Lucas N, Dominique M, Azhar S, Deroissart C, Le Sollic MA, Rondeaux J, Nobis S, Guérin C, Léon F, do Rego JC, Pons N, Le Chatelier E, Ehrlich SD, Lambert G, Déchelotte P, Fetissov SO. Commensal *Hafnia alvei* strain reduces food intake and fat mass in obese mice-a new potential probiotic for appetite and body weight management. *Int J Obes (Lond)* 44: 1041-1051, 2020.
61. Lehrskov LL, Dorph E, Widmer AM, Hepprich M, Siegenthaler J, Timper K, Donath MY. The role of IL-1 in postprandial fatigue. *Mol Metab* 12: 107-112, 2018.
62. Luck H, Tsai S, Chung J, Clemente-Casares X, Ghazarian M, Revelo XS, Lei H, Luk CT, Shi SY, Surendra A, Copeland JK, Ahn J, Prescott D, Rasmussen BA, Chng MH, Engleman EG, Girardin SE, Lam TK, Croitoru K, Dunn S, Philpott DJ, Guttman DS, Woo M, Winer S, Winer DA. Regulation of obesity-related insulin resistance with gut anti-inflammatory agents. *Cell Metab* 21: 527-42, 2015.

63. Lukowicz C, Ellero-Simatos S, Régnier M, Polizzi A, Lasserre F, Montagner A, Lippi Y, Jamin EL, Martin JF, Naylies C, Canlet C, Debrauwer L, Bertrand-Michel J, Al Saati T, Théodorou V, Loiseau N, Mselli-Lakhal L, Guillou H, Gamet-Payrastre L. Metabolic Effects of a Chronic Dietary Exposure to a Low-Dose Pesticide Cocktail in Mice: Sexual Dimorphism and Role of the Constitutive Androstane Receptor. *Environ Health Perspect* 126: 067007, 2018.
64. Macfarlane GT, Allison C, Gibson SA, Cummings JH. Contribution of the microflora to proteolysis in the human large intestine. *J Appl Bacteriol* 64: 37-46, 1988.
65. Magne J, Mariotti F, Fischer R, Mathe V, Tome D, Huneau JF. Early postprandial low-grade inflammation after high-fat meal in healthy rats: possible involvement of visceral adipose tissue. *J Nutr Biochem* 21: 550-5, 2010.
66. Mamantopoulos M, Ronchi F, Van Hauwermeiren F, Vieira-Silva S, Yilmaz B, Martens L, Saeys Y, Drexler SK, Yazdi AS, Raes J, Lamkanfi M, McCoy KD, Wullaert A. Nlrp6- and ASC-Dependent Inflammasomes Do Not Shape the Commensal Gut Microbiota Composition. *Immunity* 47: 339-348 e4, 2017.
67. Mameli C, Cattaneo C, Panelli S, Comandatore F, Sangiorgio A, Bedogni G, Bandi C, Zuccotti G, Pagliarini E. Taste perception and oral microbiota are associated with obesity in children and adolescents. *PLoS One* 14: e0221656, 2019.
68. Mazgaeen L, Gurung P. Recent Advances in Lipopolysaccharide Recognition Systems. *Int J Mol Sci* 21, 2020.
69. Mir HD, Milman A, Monnoye M, Douard V, Philippe C, Aubert A, Castanon N, Vancassel S, Guérineau NC, Naudon L, Rabot S. The gut microbiota metabolite indole increases emotional responses and adrenal medulla activity in chronically stressed male mice. *Psychoneuroendocrinology* 119: 104750, 2020.
70. Muccioli GG, Naslain D, Bäckhed F, Reigstad CS, Lambert DM, Delzenne NM, Cani PD. The endocannabinoid system links gut microbiota to adipogenesis. *Mol Syst Biol* 6: 392, 2010.

71. Naudon L, François A, Mariadassou M, Monnoye M, Philippe C, Bruneau A, Dussauze M, Rué O, Rabot S, Meunier N. First step of odorant detection in the olfactory epithelium and olfactory preferences differ according to the microbiota profile in mice. *Behav Brain Res* 384: 112549, 2020.
72. Neurath MF. Cytokines in inflammatory bowel disease. *Nat Rev Immunol* 14: 329-42, 2014.
73. Nuzzaci D, Cansell C, Lienard F, Nedelec E, Ben Fradj S, Castel J, Foppen E, Denis R, Grouselle D, Laderriere A, Lemoine A, Mathou A, Tolle V, Heurtaux T, Fioramonti X, Audinat E, Penicaud L, Nahon JL, Rovere C, Benani A. Postprandial Hyperglycemia Stimulates Neuroglial Plasticity in Hypothalamic POMC Neurons after a Balanced Meal. *Cell Rep* 30: 3067-3078 e5, 2020.
74. Overduin J, Schoterman MH, Calame W, Schonewille AJ, Ten Bruggencate SJ. Dietary galacto-oligosaccharides and calcium: effects on energy intake, fat-pad weight and satiety-related, gastrointestinal hormones in rats. *Br J Nutr* 109: 1338-48, 2013.
75. Pais de Barros JP, Gautier T, Sali W, Adrie C, Choubley H, Charron E, Lalande C, Le Guern N, Deckert V, Monchi M, Quenot JP, Lagrost L. Quantitative lipopolysaccharide analysis using HPLC/MS/MS and its combination with the limulus amebocyte lysate assay. *J Lipid Res* 56: 1363-9, 2015.
76. Parnell JA, Reimer RA. Weight loss during oligofructose supplementation is associated with decreased ghrelin and increased peptide YY in overweight and obese adults. *Am J Clin Nutr* 89: 1751-9, 2009.
77. Qiang X, Liotta AS, Shiloach J, Gutierrez JC, Wang H, Ochani M, Ochani K, Yang H, Rabin A, LeRoith D, Lesniak MA, Bohm M, Maaser C, Kannengiesser K, Donowitz M, Rabizadeh S, Czura CJ, Tracey KJ, Westlake M, Zarfeshani A, Mehdi SF, Danoff A, Ge X, Sanyal S, Schwartz GJ, Roth J. New melanocortin-like peptide of *E. coli* can suppress inflammation via the mammalian melanocortin-1 receptor (MC1R): possible endocrine-like function for microbes of the gut. *NPJ Biofilms Microbiomes* 3: 31, 2017.

78. Rastelli M, Knauf C, Cani PD. Gut Microbes and Health: A Focus on the Mechanisms Linking Microbes, Obesity, and Related Disorders. *Obesity (Silver Spring)* 26: 792-800, 2018.
79. Rathinam VA, Fitzgerald KA. Inflammasome Complexes: Emerging Mechanisms and Effector Functions. *Cell* 165: 792-800, 2016.
80. Rheinheimer J, de Souza BM, Cardoso NS, Bauer AC, Crispim D. Current role of the NLRP3 inflammasome on obesity and insulin resistance: A systematic review. *Metabolism* 74: 1-9, 2017.
81. Richard CD, Tolle V, Low MJ. Meal pattern analysis in neural-specific proopiomelanocortin-deficient mice. *Eur J Pharmacol* 660: 131-8, 2011.
82. Sanchez M, Darimont C, Panahi S, Drapeau V, Marette A, Taylor VH, Dore J, Tremblay A. Effects of a Diet-Based Weight-Reducing Program with Probiotic Supplementation on Satiety Efficiency, Eating Behaviour Traits, and Psychosocial Behaviours in Obese Individuals. *Nutrients* 9, 2017.
83. Sha T, Sunamoto M, Kitazaki T, Sato J, Ii M, Iizawa Y. Therapeutic effects of TAK-242, a novel selective Toll-like receptor 4 signal transduction inhibitor, in mouse endotoxin shock model. *Eur J Pharmacol* 571: 231-9, 2007.
84. Sisley S, Gutierrez-Aguilar R, Scott M, D'Alessio DA, Sandoval DA, Seeley RJ. Neuronal GLP1R mediates liraglutide's anorectic but not glucose-lowering effect. *J Clin Invest* 124: 2456-63, 2014.
85. So PW, Yu WS, Kuo YT, Wasserfall C, Goldstone AP, Bell JD, Frost G. Impact of resistant starch on body fat patterning and central appetite regulation. *PLoS One* 2: e1309, 2007.
86. Thaïss CA, Zeevi D, Levy M, Zilberman-Schapira G, Suez J, Tengeler AC, Abramson L, Katz MN, Korem T, Zmora N, Kuperman Y, Biton I, Gilad S, Harmelin A, Shapiro H, Halpern Z, Segal E, Elinav E. Transkingdom control of microbiota diurnal oscillations promotes metabolic homeostasis. *Cell* 159: 514-29, 2014.

87. Tolhurst G, Heffron H, Lam YS, Parker HE, Habib AM, Diakogiannaki E, Cameron J, Grosse J, Reimann F, Gribble FM. Short-chain fatty acids stimulate glucagon-like peptide-1 secretion via the G-protein-coupled receptor FFAR2. *Diabetes* 61: 364-71, 2012.
88. Tremaroli V, Backhed F. Functional interactions between the gut microbiota and host metabolism. *Nature* 489: 242-9, 2012.
89. van de Wouw M, Schellekens H, Dinan TG, Cryan JF. Microbiota-Gut-Brain Axis: Modulator of Host Metabolism and Appetite. *J Nutr* 147: 727-745, 2017.
90. Vors C, Pineau G, Draï J, Meugnier E, Pesenti S, Laville M, Laugerette F, Malpuech-Brugere C, Vidal H, Michalski MC. Postprandial Endotoxemia Linked With Chylomicrons and Lipopolysaccharides Handling in Obese Versus Lean Men: A Lipid Dose-Effect Trial. *J Clin Endocrinol Metab* 100: 3427-35, 2015.
91. Wichmann A, Allahyar A, Greiner TU, Plovier H, Lunden GO, Larsson T, Drucker DJ, Delzenne NM, Cani PD, Backhed F. Microbial modulation of energy availability in the colon regulates intestinal transit. *Cell Host Microbe* 14: 582-90, 2013.
92. Zarrinpar A, Chaix A, Xu ZZ, Chang MW, Marotz CA, Saghatelian A, Knight R, Panda S. Antibiotic-induced microbiome depletion alters metabolic homeostasis by affecting gut signaling and colonic metabolism. *Nat Commun* 9: 2872, 2018.
93. Zorrilla EP, Inoue K, Fekete EM, Tabarin A, Valdez GR, Koob GF. Measuring meals: structure of prandial food and water intake of rats. *Am J Physiol Regul Integr Comp Physiol* 288: R1450-67, 2005.

Legends

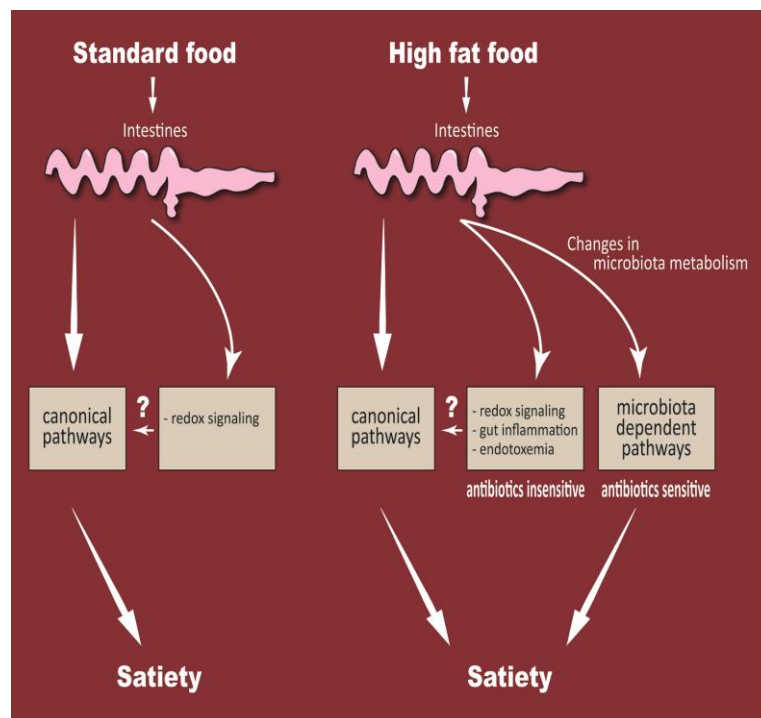


Figure 1. Schematic representation of constitutive microbiota-dependent short-term control of food intake in mice.

The constitutive gut microbiota controls host appetite at the time scale of a meal under normal physiology. The antibiotic-sensitive microbiota-derived anorectic effect develops specifically with a high-fat food.

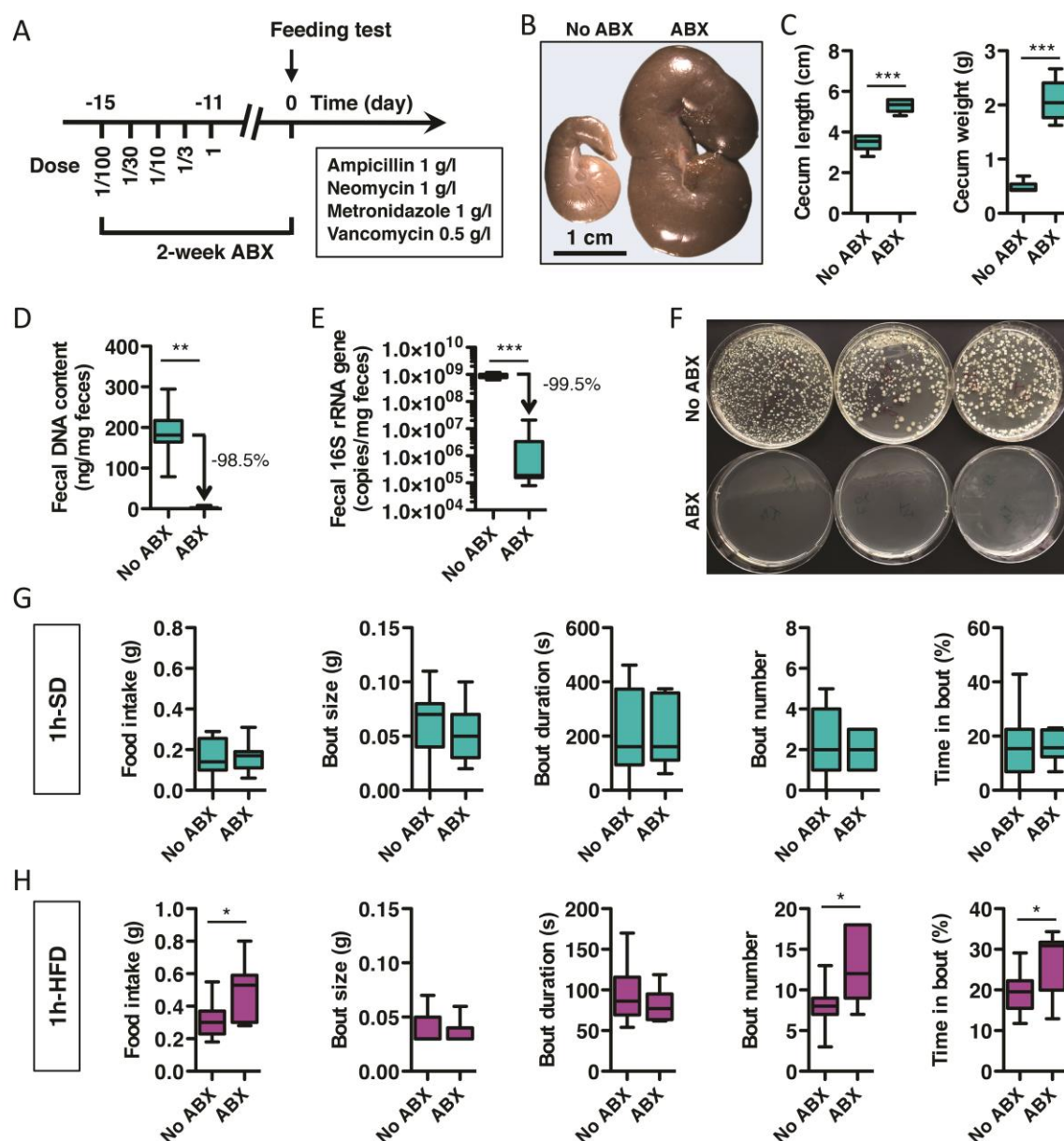


Figure 2. Microbiota depletion by long-term broad-spectrum antibiotics (ABX) alters feeding behavior in mice when consuming high-fat food.

(A) Dose of antibiotics.

(B) Representative cecum from ABX-treated mouse (right) and a non-treated mouse (left).

(C) Length and weight of ceca from mice treated or not treated with antibiotics (n=6 mice/group).

(D) DNA content in the feces of mice treated or not treated with antibiotics (No ABX: n=9 mice; ABX: n=7 mice).

(E) Number of copies of the gene coding for 16S rRNA in the feces of mice after ABX treatment (No ABX, n=9 mice; ABX, n=7 mice).

(F) Fecal cultures from mice treated or not treated with antibiotics (No ABX, n=3 mice; ABX, n=3 mice).

(G, H) Feeding behavior including cumulative food intake, size of feeding bouts, duration of feeding bouts, number of feeding bouts and percentage of time spent in bouts over a 60-min period in mice treated or not treated with antibiotics, and exposed to standard diet (H) or high-fat diet (I) (No ABX: n=9 mice; ABX: n=7 mice).

Data were analyzed using the Mann-Whitney test. Asterisks indicate statistical differences between groups: * $p < 0.05$, ** $p < 0.01$, and *** $p < 0.001$.

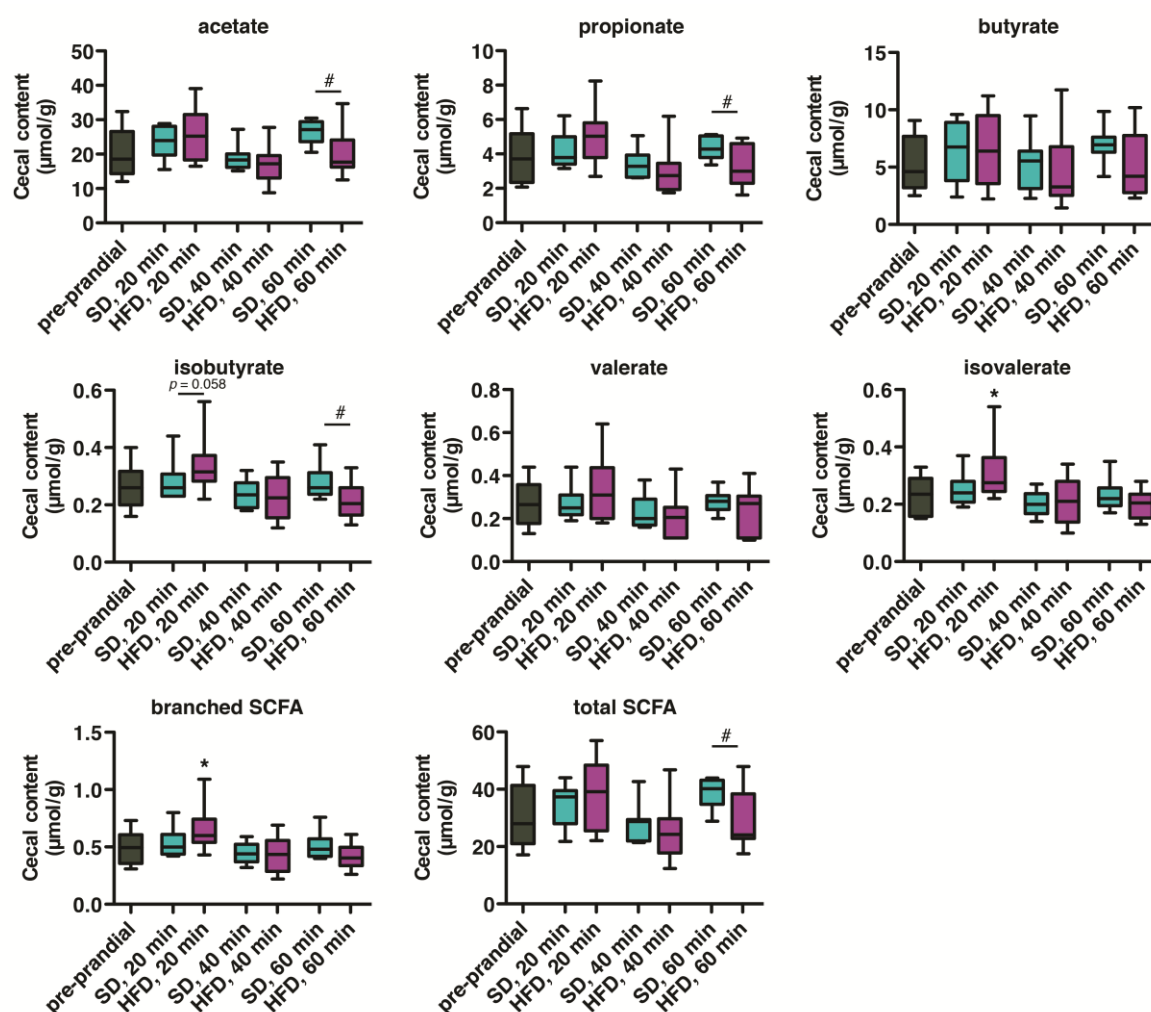


Figure 3. Postprandial changes in microbial metabolites in the cecum in mice within one hour of consumption of either standard or high-fat food.

Concentration of acetate, propionate, butyrate, isobutyrate, valerate, isovalerate, branched SCFA and total SCFA, in ceca of mice during the preprandial state and in mice fed a SD or HFD for 20 min, 40 min or 60 min. Concentrations were measured by gas chromatography (n=10 mice per time point).

Data were analyzed using the Mann-Whitney test. Symbols indicate statistical differences between groups: * p < 0.05 (preprandial vs HFD), # p < 0.05 (SD vs HFD).

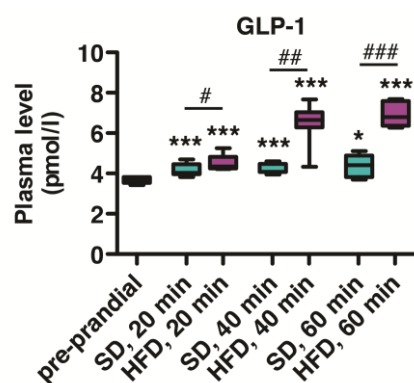


Figure 4. Postprandial GLP-1 response in mice within one hour after consumption of either standard or high-fat food.

Plasma levels of total GLP-1 in mice in a preprandial state or in mice fed SD or HFD for 20 min, 40 min or 60 min (n=8-9 mice/group).

Data were analyzed with the Mann-Whitney test. Symbols indicate statistical differences between groups: * $p < 0.05$ and *** $p < 0.001$ (preprandial vs HFD), # $p < 0.05$, ## $p < 0.01$, and ### $p < 0.001$ for $p < 0.05$ (SD vs HFD).

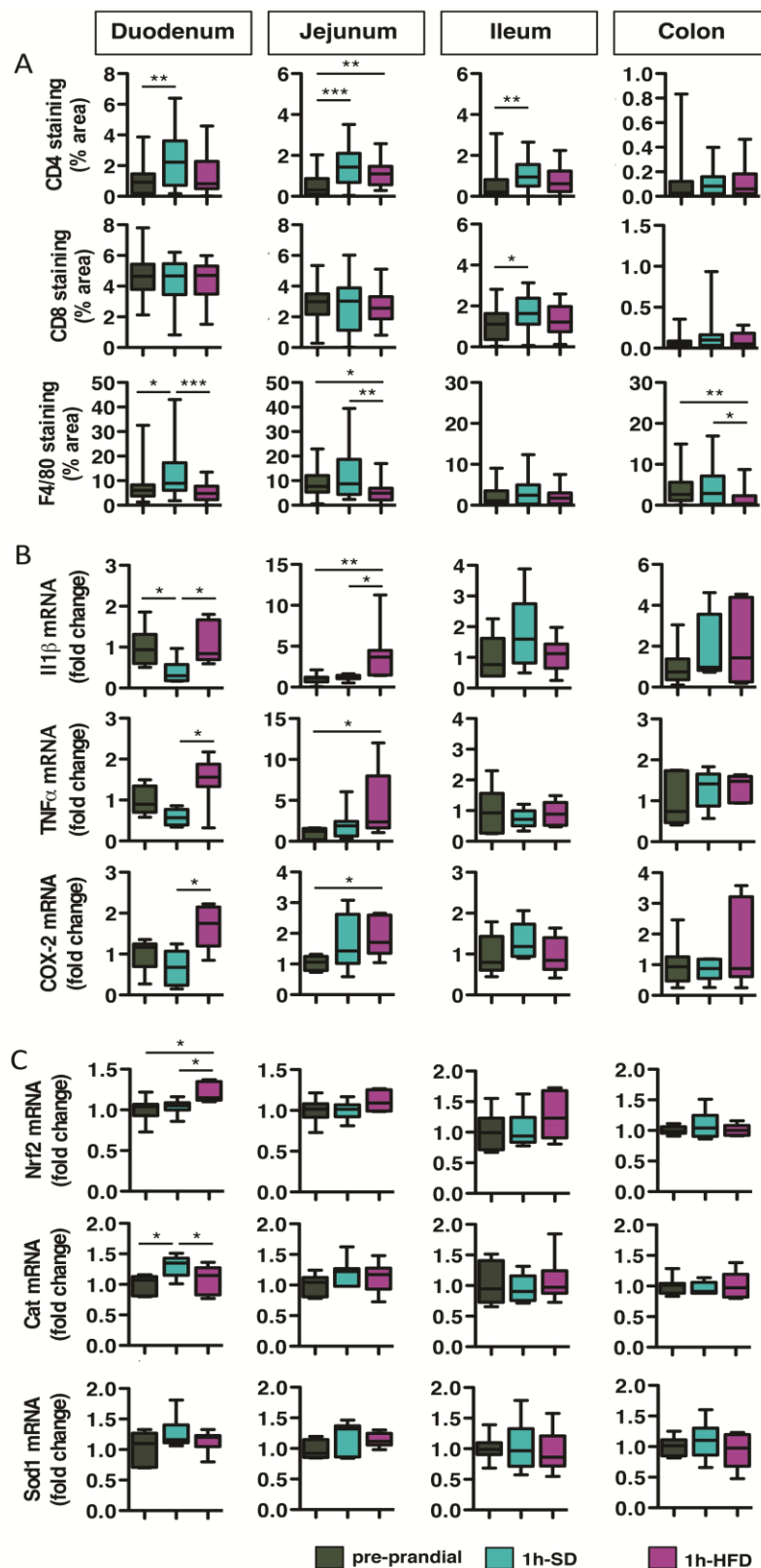


Figure 5. Postprandial inflammatory response in the gut in mice after consumption of either standard or high-fat food for one hour.

(A) Immunohistochemical detection of CD4, CD8 and F4/80 epitopes in the duodenum, jejunum, ileum and colon of mice during the preprandial state and in mice fed SD or HFD for 1 h. Expression levels are shown as a percentage of stained area (n=7 mice/group with n=4 images/tissue/mouse).

(B, C) Relative expression of pro-inflammatory IL-1 β , TNF α , COX-2 (B), and redox markers NRF2, CAT, SOD-1 mRNA (C), in the duodenum, jejunum, ileum and colon of mice during the preprandial state and in mice fed SD or HFD for 1 h (n=7 mice/group). Levels were measured by RT-qPCR.

Data were analyzed with ANOVA and Newman-Keuls tests. Asterisks indicate statistical differences between groups: *p<0.05, **p<0.01, and ***p<0.001.

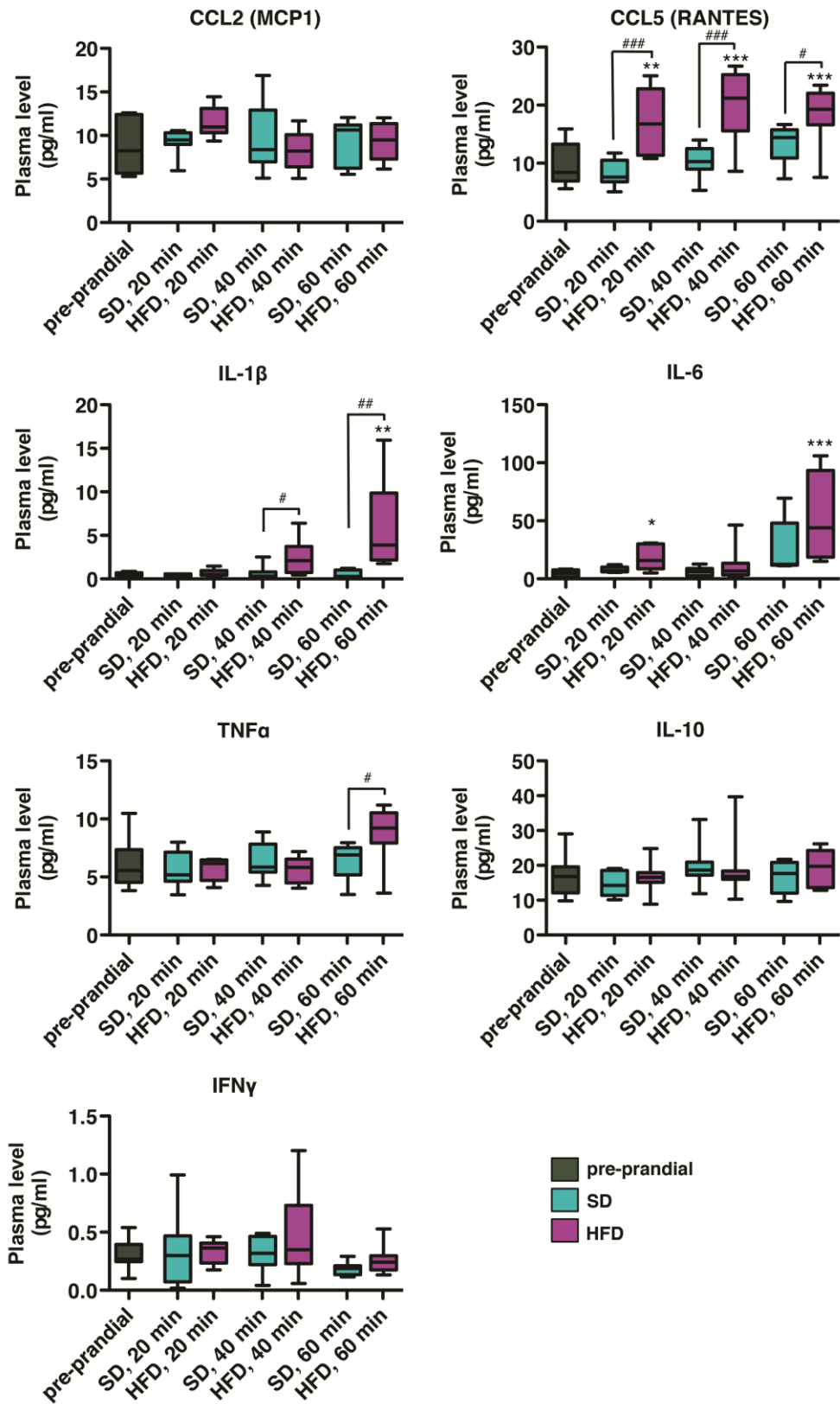


Figure 6. Postprandial inflammatory response in the blood of mice within one hour of consumption of either standard or high-fat food.

Plasma levels of CCL2, CCL5, IL-1 β , IL-6, TNF α , IL-10 and IFN γ were measured in mice in a preprandial state or in mice fed a SD or HFD for 20 min, 40 min or 60 min (n=8-9 mice/group).

Data were analyzed with the Mann-Whitney test. Symbols indicate statistical differences between groups: *p<0.05, **p<0.01, and ***p<0.001 (preprandial vs HFD), # p<0.05, ## p<0.01, and ### p<0.001 for p<0.05 (SD vs HFD).

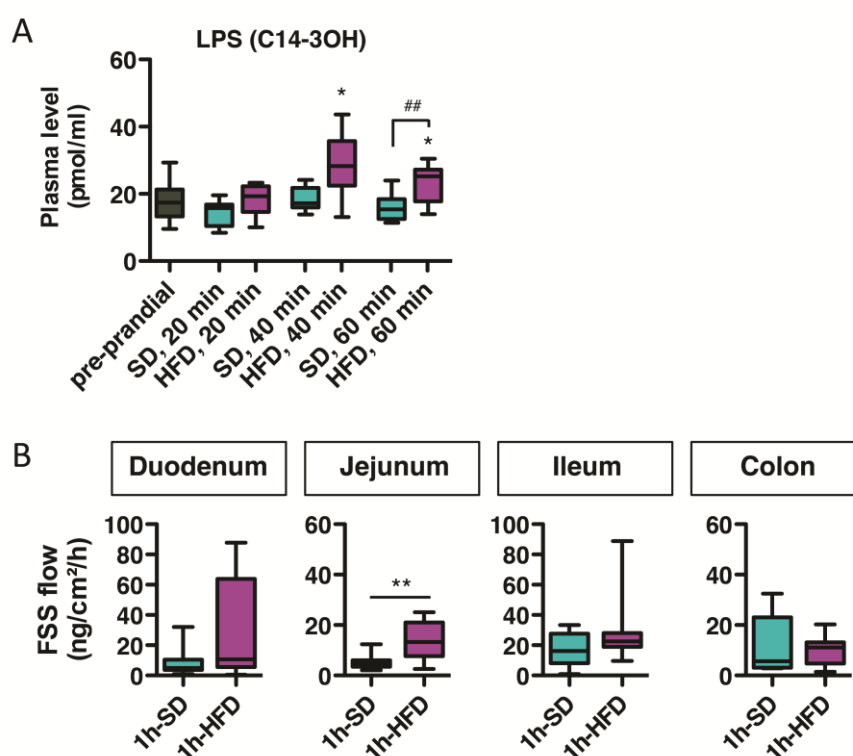
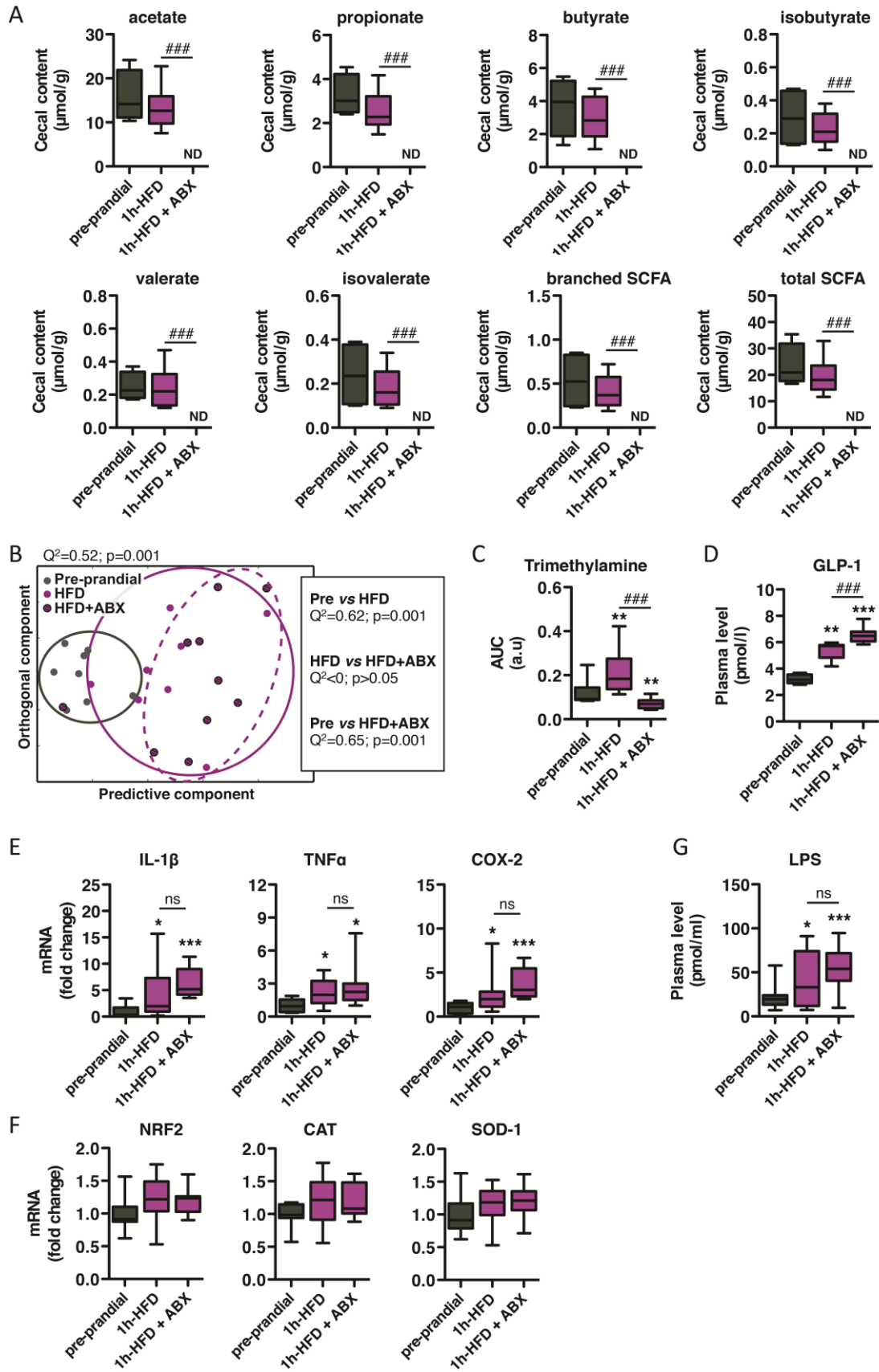


Figure 7. Characterization of the systemic postprandial endotoxemic response and gut permeability in mice within one hour of consumption of either a standard or a high-fat diet.

(A) Plasma levels of LPS-derived esterified 3-hydroxymyristic acid in mice in a preprandial state or in mice fed a SD or HFD for 20 min, 40 min or 60 min (n=8-9 mice/group).

(B) Permeability for 0.38 kDa fluorescent sodium salt (FSS) in the duodenum, jejunum, ileum and colon biopsies from mice fed SD or a HFD for 60 min (n=8 mice/group).

For the LPS analysis, data were analyzed with ANOVA and Newman-Keuls tests. Symbols indicate statistical differences between groups: * $p < 0.05$ (preprandial vs HFD), ## $p < 0.01$, (SD vs HFD). For gut permeability analysis, data were analyzed using a Mann-Whitney test. Asterisks indicate statistical differences between groups: ** $p < 0.01$.



(A) Concentrations of acetate, propionate, butyrate, isobutyrate, valerate, isovalerate, branched SCFA and total SCFA, in the cecum of mice in the preprandial state (pre), in mice fed a HFD for 1 hour (1h-HFD), and in mice treated with antibiotics and fed a HFD for 1 hour (1h-HFD + ABX) (pre: n=4 mice; 1h-HFD: n=9 mice, 1h-HFD + ABX: n=9 mice).

(B) Orthogonal projection on latent structure-discriminant analysis (O-PLS-DA) score plots derived from the ^1H -NMR-based plasma spectra. Q^2Y represents the goodness of fit for the PLS-DA models, and p -values were derived using 1,000 permutations of the Y matrix.

(C) Levels of plasma trimethylamine of mice in the preprandial state (pre), in mice fed HFD for 1 hour (1h-HFD), and in mice treated with antibiotics and fed HFD for 1 hour (1h-HFD + ABX) (pre: n=9 mice; 1h-HFD: n=9, 1h-HFD + ABX: n=10 mice).

(D) Total GLP-1 in plasma of mice in the preprandial state (pre), in mice fed HFD for 1 hour (1h-HFD), and in mice treated with antibiotics and fed HFD for 1 hour (1h-HFD + ABX) (pre: n=5 mice; 1h-HFD: n=6, 1h-HFD + ABX: n=10 mice).

(E, F) Pro-inflammatory (E) and redox (F) markers in the jejunum of mice in the preprandial state (pre), in mice fed a HFD for 1 hour (1h-HFD), and in mice treated with antibiotics and fed a HFD for 1 hour (1h-HFD + ABX). Relative expressions of IL-1 β , TNF α , COX-2, NRF2, CAT and SOD-1 mRNA were measured by RT-qPCR (pre: n=9 mice; 1h-HFD: n=9, 1h-HFD + ABX: n=10 mice).

(G) Plasma levels of LPS-derived esterified 3-hydroxymyristic acid in mice in the preprandial state (pre), in mice fed a HFD for 1 hour (1h-HFD), and in mice treated with antibiotics and fed a HFD for 1 hour (1h-HFD + ABX) (pre: n=9 mice; 1h-HFD: n=9, 1h-HFD + ABX: n=10 mice).

In (B), each data point represents an individual mouse.

Data were analyzed using the Mann-Whitney test. Symbols indicate statistical differences between groups: * $p < 0.05$, ** $p < 0.01$ and *** $p < 0.001$ (preprandial vs HFD), # $p < 0.05$, ## $p < 0.01$, and ### $p < 0.001$ for $p < 0.05$ (SD vs HFD).

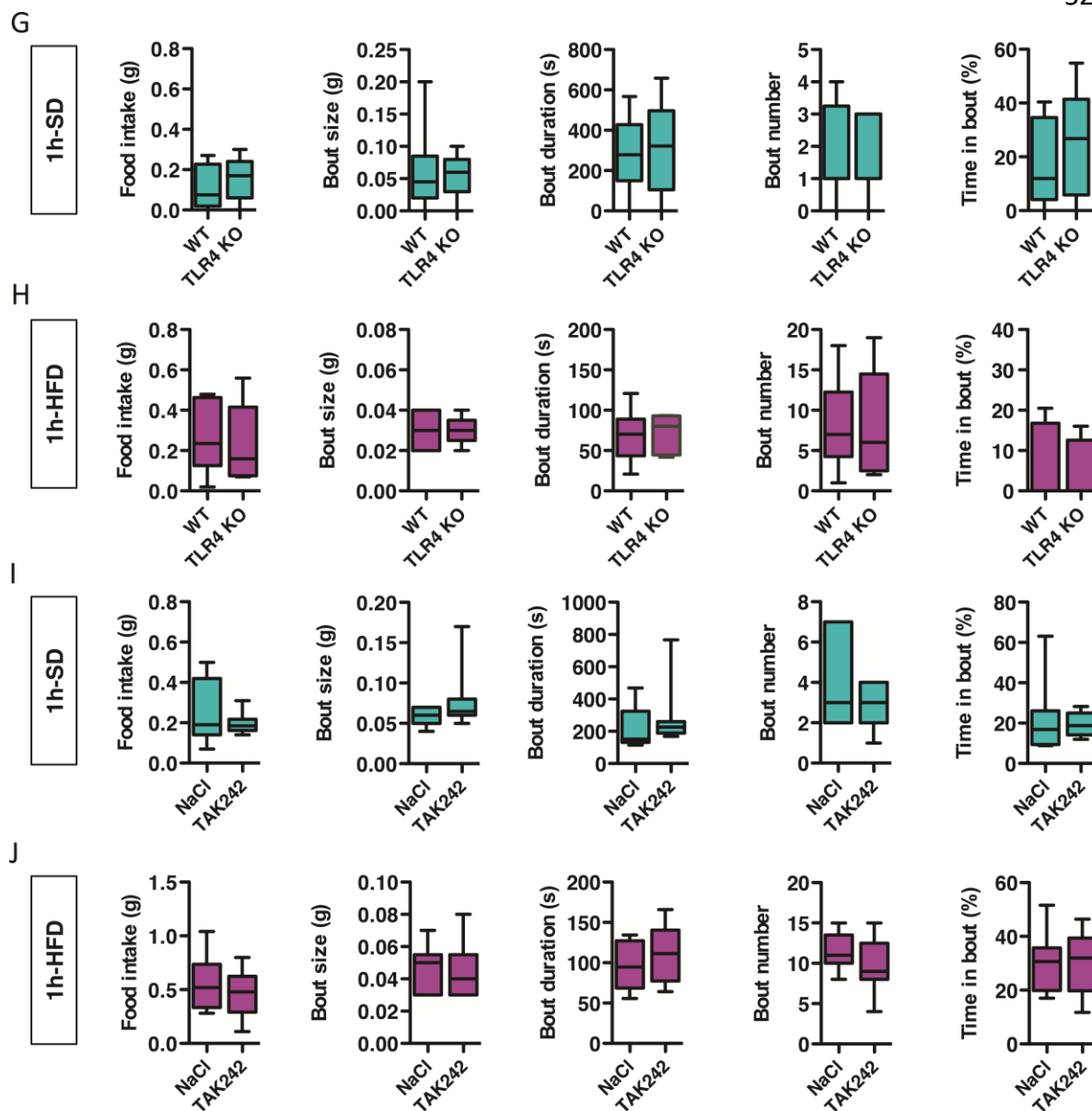


Figure 9. NLRP3-inflammasome and TLR4 receptors are not involved in the short-term regulation of food intake.

(A, B) Feeding behavior including cumulative food intake, size of feeding bouts, duration of feeding bouts, number of feeding bouts and percentage of time spent in bouts during a 60 min-period in wild-type and ASC-KO mice exposed to standard diet (A) or high-fat diet (B) (WT: n=10 mice; ASC-KO: n=10 mice).

(C, D) Feeding behavior over a 60 min-period in wild-type and NLRP3-KO mice with standard diet (C) or high-fat diet (D) (WT: n=6 mice; ASC-KO: n=9 mice).

(E, F) Feeding behavior over a 60 min-period in mice treated with NaCl or MCC950 and fed a standard diet (E) or high-fat diet (F) (NaCl: n=8 mice; MCC950: n=7 mice).

(G, H) Feeding behavior including cumulative food intake, size of feeding bouts, duration of feeding bouts, number of feeding bouts and percentage of time spent in bouts during a 60 min-period in wild-type and TLR4-KO mice exposed to standard diet (A) or high-fat diet (B) (WT: n=10 mice; TLR4-KO: n=5 mice).

(I, J) Feeding behavior during a 60 min-period in mice treated with NaCl or TAK-242 and fed a standard diet (C) or high-fat diet (D) (NaCl: n=9 mice; TAK-242: n=9 mice).

Data were analyzed using the Mann-Whitney test.